Terahertz Spectroscopy in the Laboratory and in Space

T. Amano

Department of Chemistry

and

Department of Physics and Astronomy

The University of Waterloo

In this talk……….

- Sub-mm (THz) spectrometer
- Example of interplay between lab spectroscopy and astronomical observation

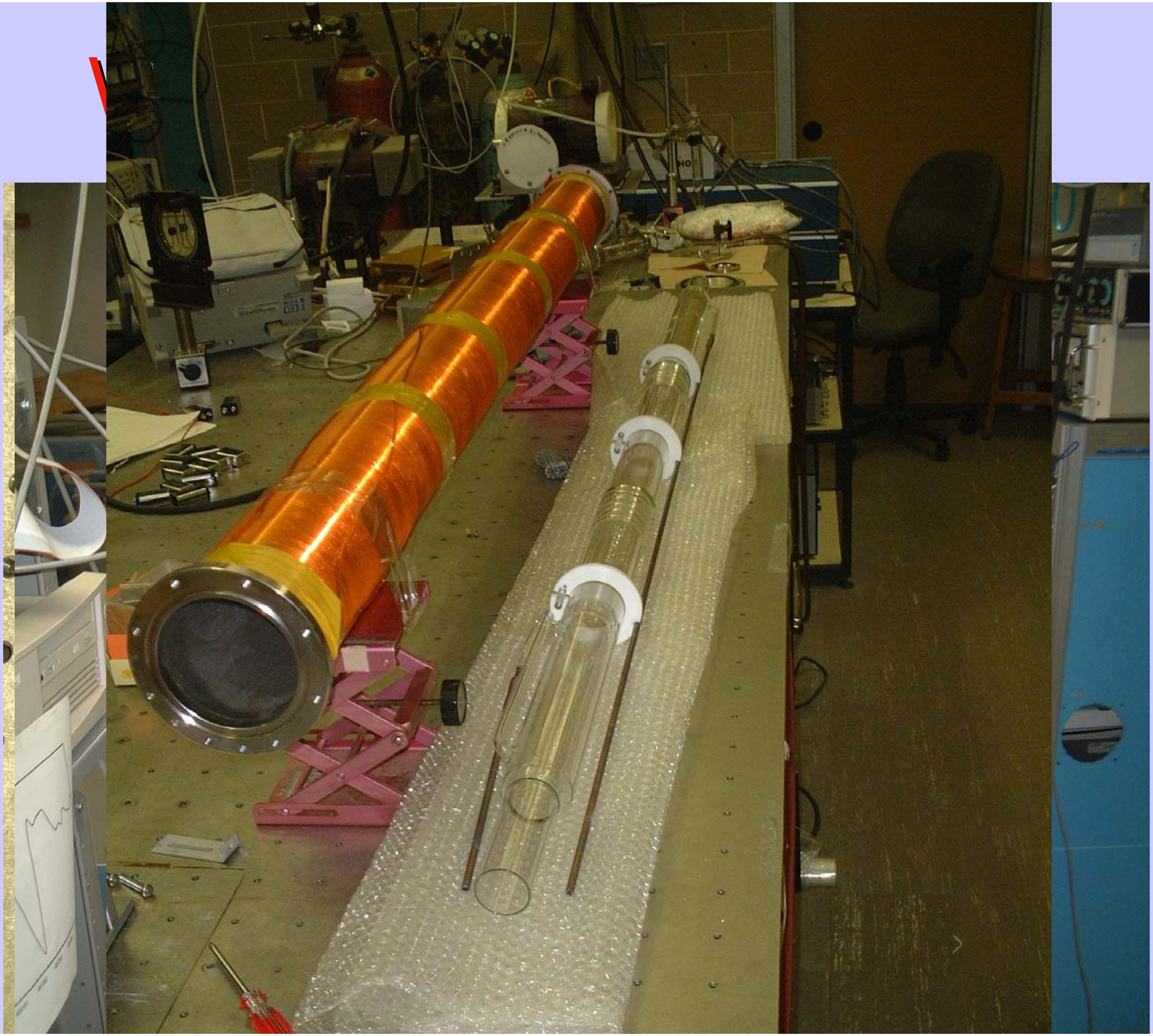

Double modulation sub-mm system at Waterloo

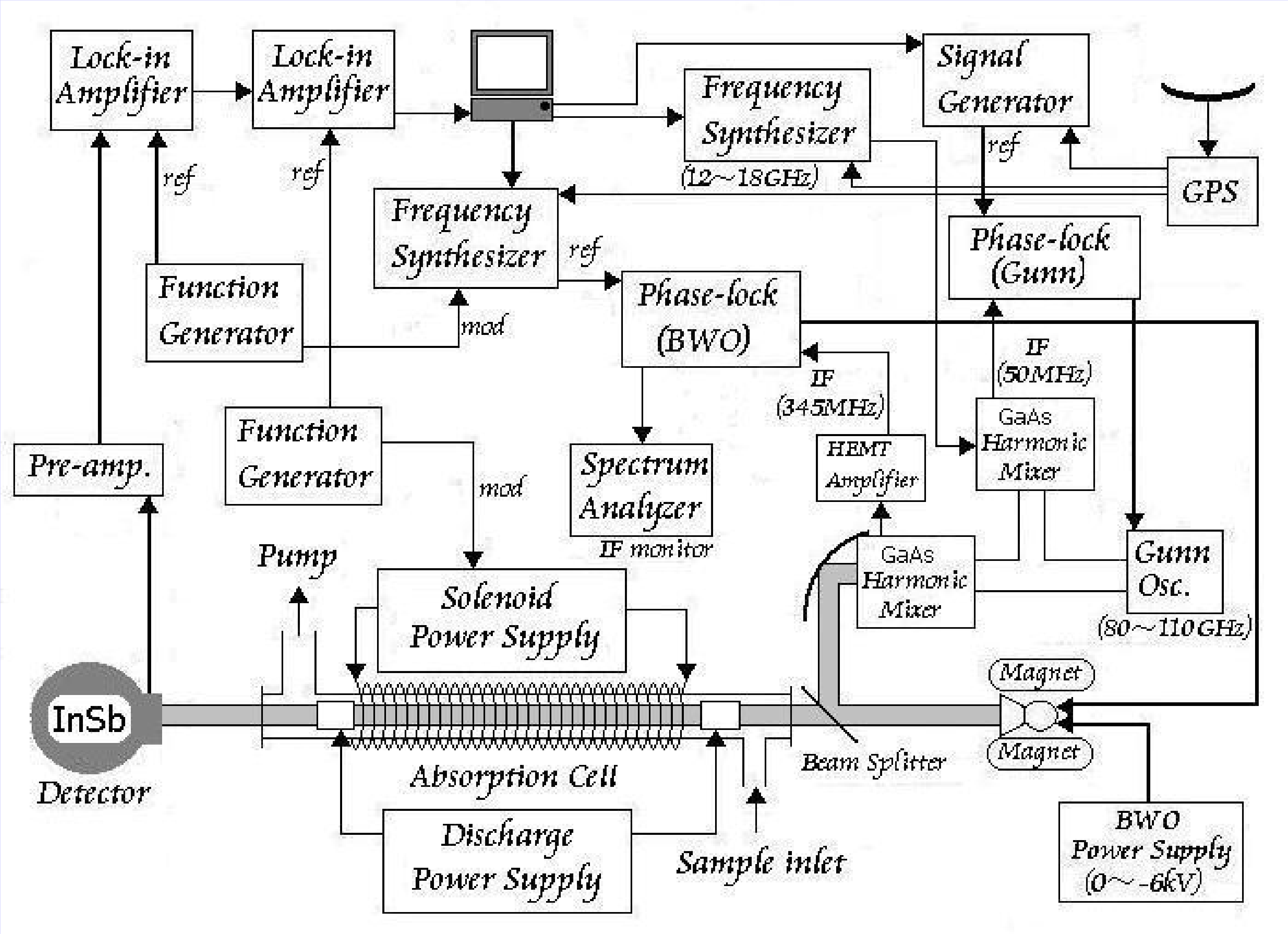

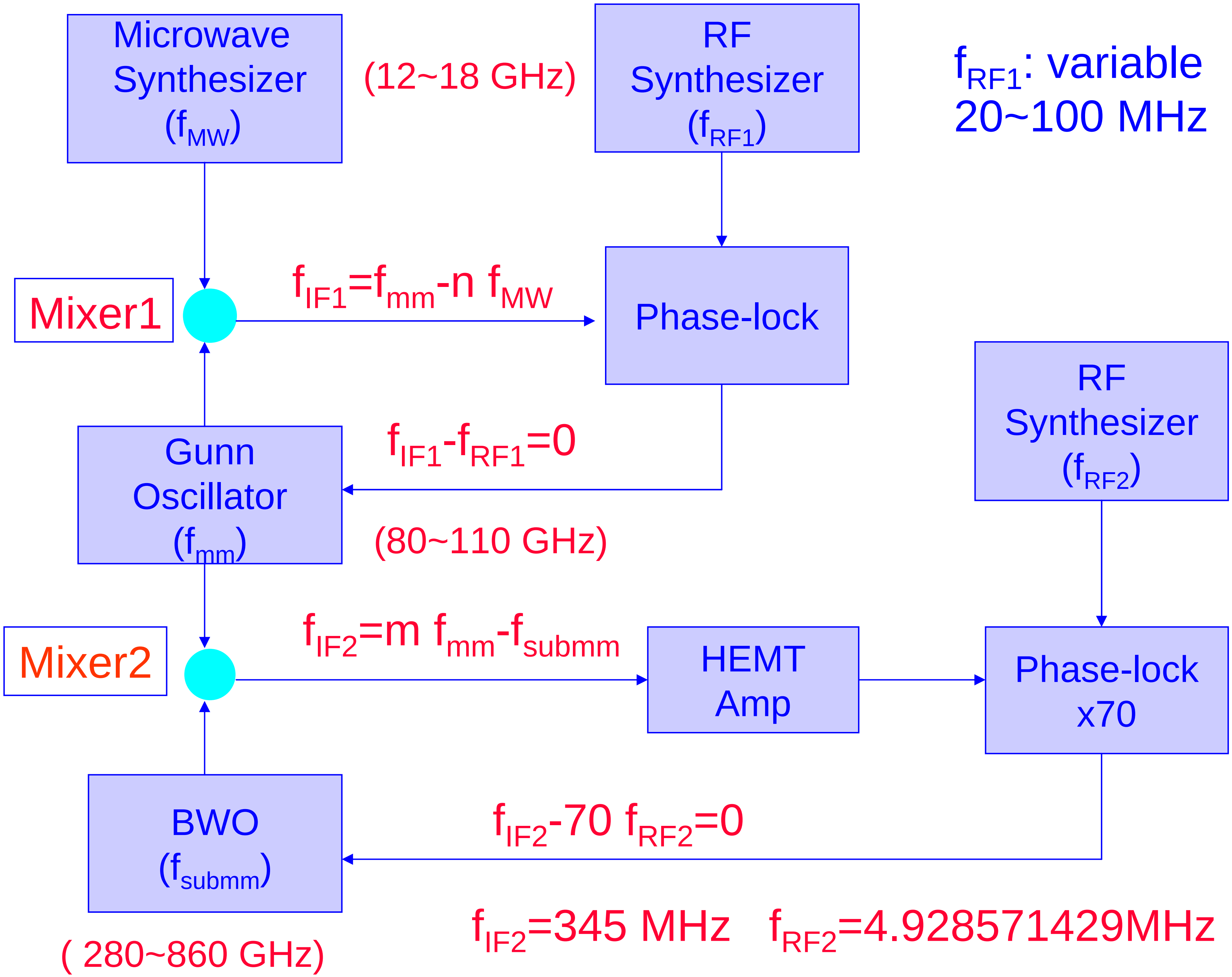
Microwave Synthesizer (f_{MW})
(12~18 GHz)
RF Synthesizer (f_{RF1})
f_{RF1}: variable
20~100 MHz
Mixer1
$f_{IF1}=f_{mm}-n\ f_{MW}$
Phase-lock
RF Synthesizer (f_{RF2})
Gunn Oscillator (f_{mm})
$f_{IF1}-f_{RF1}=0$
(80~110 GHz)
Mixer2
$f_{IF2}=m\ f_{mm}-f_{submm}$
HEMT Amp
Phase-lock x70
BWO (f_{submm})
$f_{IF2}-70\ f_{RF2}=0$
(280~860 GHz)
$f_{IF2}=345$ MHz
$f_{RF2}=4.928571429$MHz

Three types of discharges are tri... ...nstable ...s

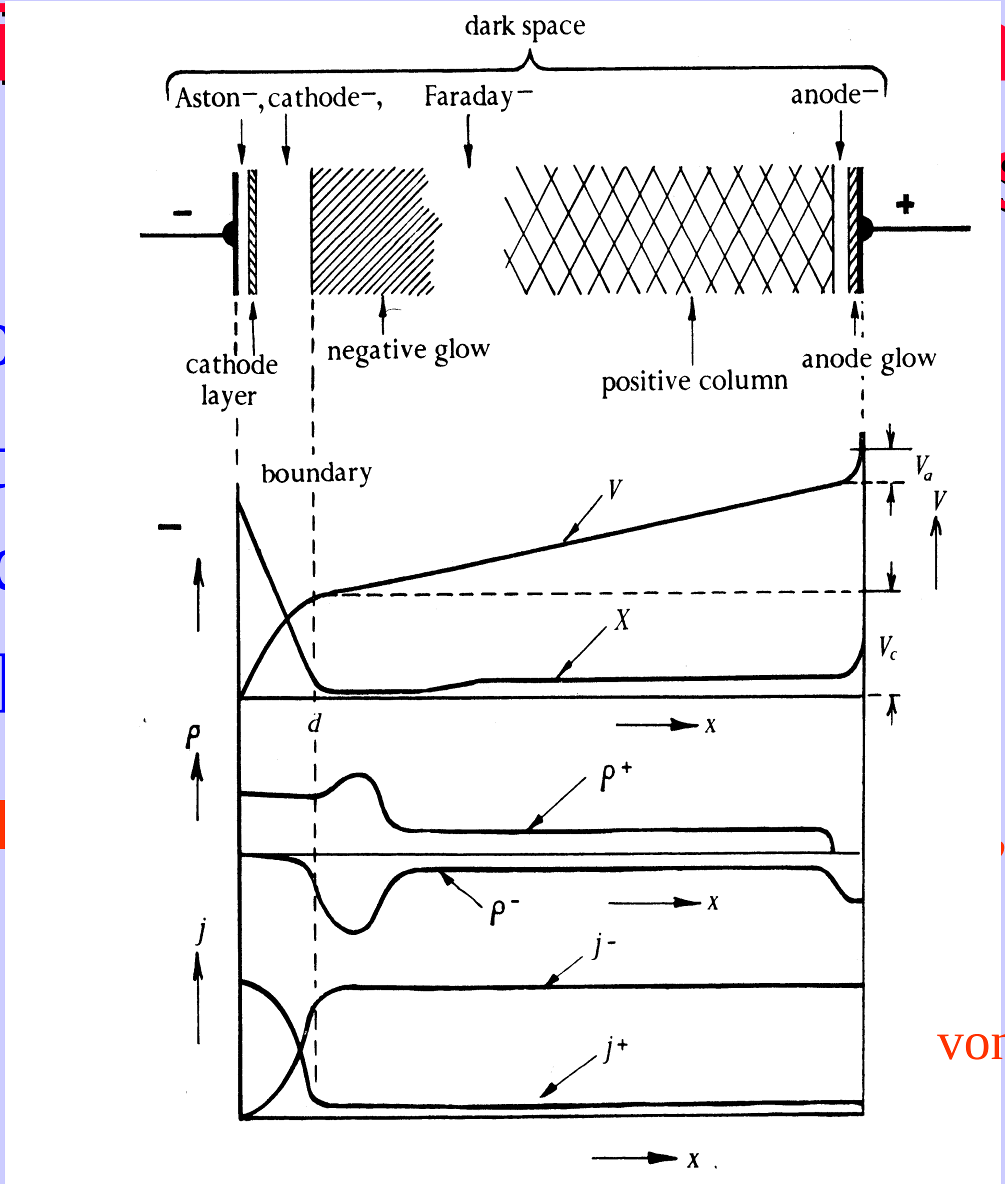

- Glo...
- Ext... disc...
- Hol...

I... , 2312 (1983)

von Engel "Ionized Gases"

Discovery of multiply deuterated species in space

$[D]/[H] \sim 1.5\times10^{-5}$

D_2CO :	Turner(1990)	Ori-KL	0.3%
	Ceccarelli *et al* (1998)	IRAS 16293-2422	5%
	Loinard *et al* (2001)	16293E	26%

NHD_2 (2000) , ND_3 (2002)

CHD_2OH (2002), CD_3OH (2004)

D_2S (2003)

Formation of Deuterated Species

- H/D exchange reactions of H_3^+ with HD are exothermic.

$$H_3^+ + HD \rightarrow H_2D^+ + H_2 + 230\ K$$

$$H_2D^+ + HD \rightarrow D_2H^+ + H_2 + 180\ K$$

$$D_2H^+ + HD \rightarrow D_3^+ + H_2 + 230\ K$$

Under liquid-N_2 cooled environment , such reactions become dominant.

Roberts, Herbst, and Millar, *Astrophys J*. **591**, L41 (2003)

Spectroscopy of H_2D^+ and D_2H^+

IR

- Shy, Farley, Wing (1981): Ion beam
- Amano & Watson (1984), Amano (1985): ν_1 band (H_2D^+)
- Lubic & Amano (1984): ν_1 band (D_2H^+)
- Foster et al. (1986): ν_2 /ν_3 bands (H_2D^+)
- Foster, McKellar, Watson. (1986): ν_2 /ν_3 bands (D_2H^+)
- Polyansky & McKellar (1990): All available data were fitted together to improve molecular constants. (D_2H^+)
- Fárník et al. (2002):

  Molecular beam experiments of vibrational overtone and combination bands ($2\nu_2$, $2\nu_3$, $\nu_2+\nu_3$).

mm-, sub-mm, FIR

- Bogey et al. (1984): 1_{10}-1_{11} H_2D^+ (372.4 GHz)
  Warner et al.(1984):
- Saito, Kawaguchi, Hirota (1985): 2_{20}-2_{21} H_2D^+ (156.0 GHz)
- Jennings, Demuynck, Banek, Evenson (unpublished):
  1_{01}-0_{00} H_2D^+ (1370.1 GHz)
  1_{11}-0_{00} D_2H^+ (1476.6 GHz)
  2_{20}-2_{11} D_2H^+ (1370.1 GHz)
- Hirao & Amano (2003): 1_{10}-1_{01} D_2H^+ (691.7 GHz)
- Amano & Hirao (2005): 3_{21}-3_{22} H_2D^+ (646.4 GHz)

Energy Level Diagram of H_2D^+

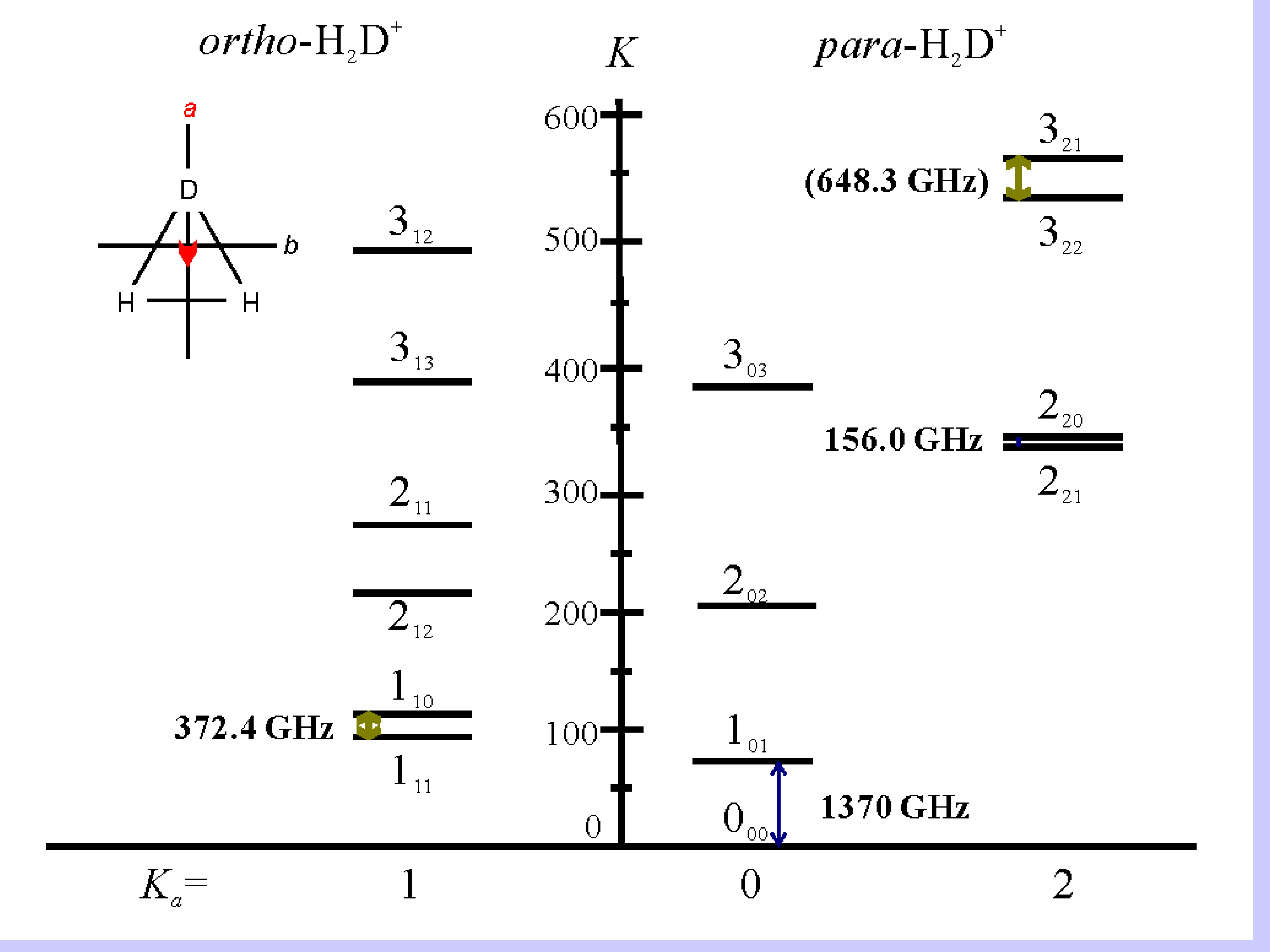

Energy Level Diagram of D_2H^+

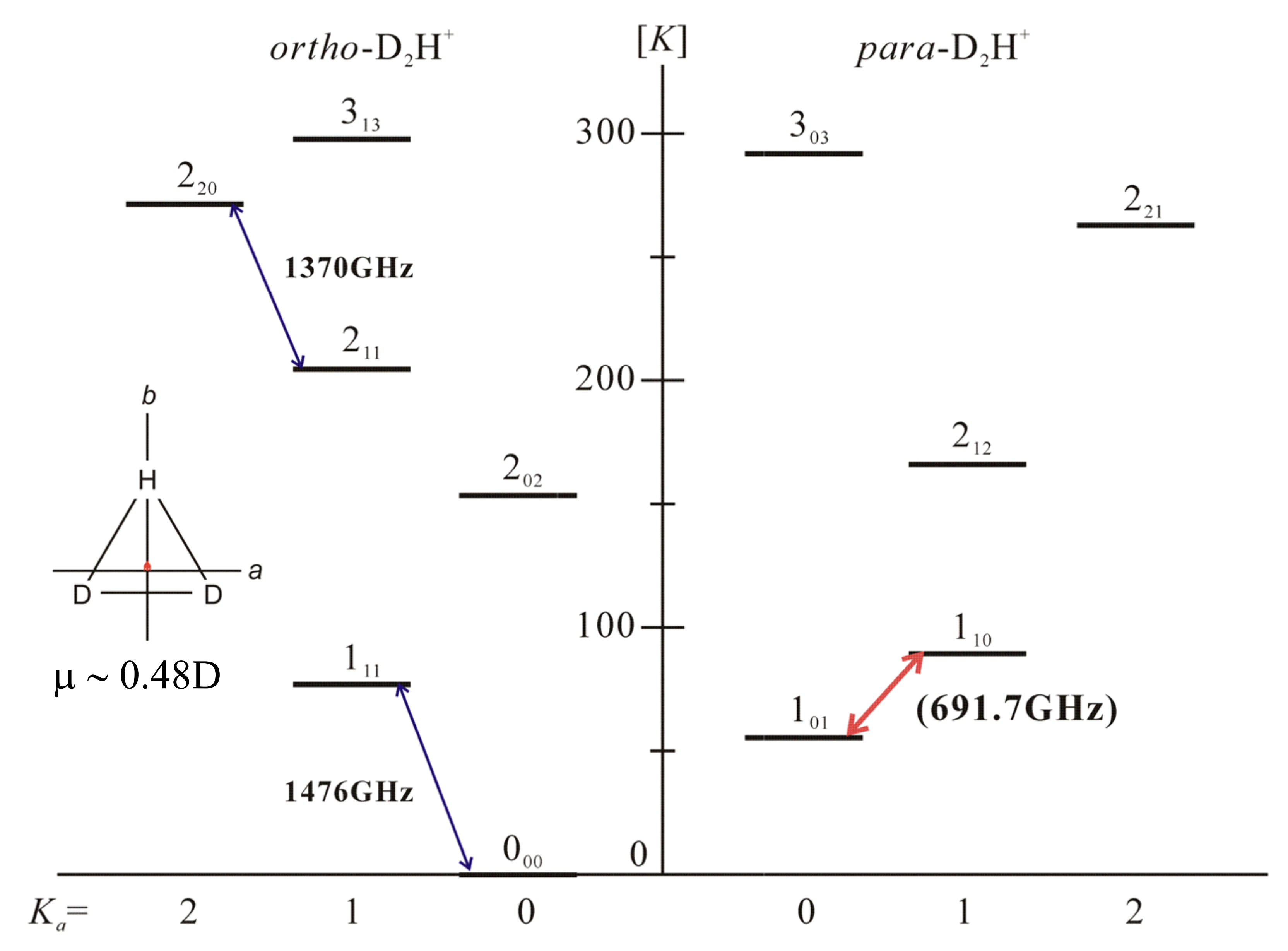

Experimental Details

- Extended negative glow discharge source.
  (Magnetic field: 200G).
- Double modulation.
- $H_2/D_2/Ar$ = 3 /2 /17 mTorr, I = 8 mA,
  T ~ 77 K

↓

Search around 691.705 (90) GHz.

(Polyansky and McKellar)

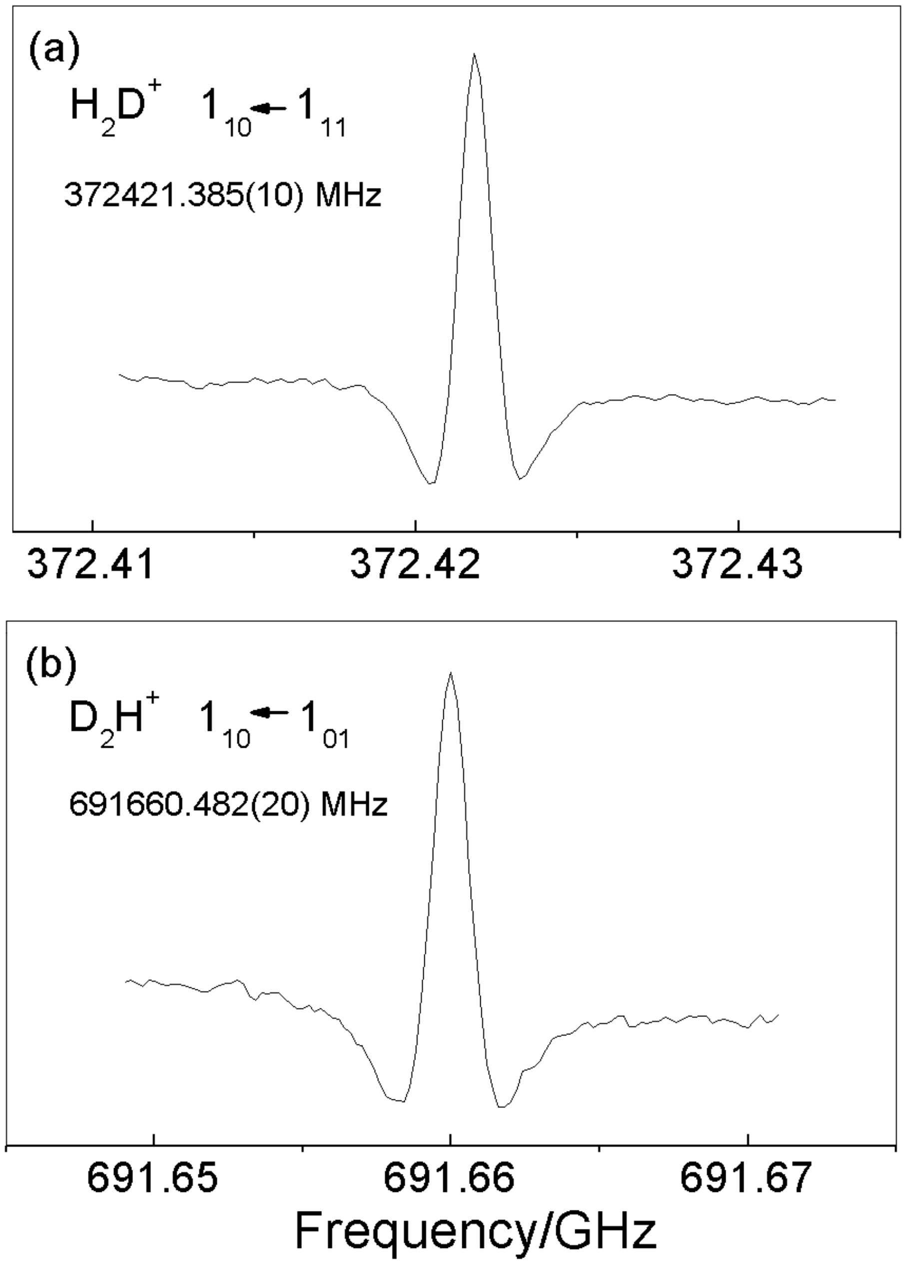

Laboratory observations of H_2D^+ and D_2H^+

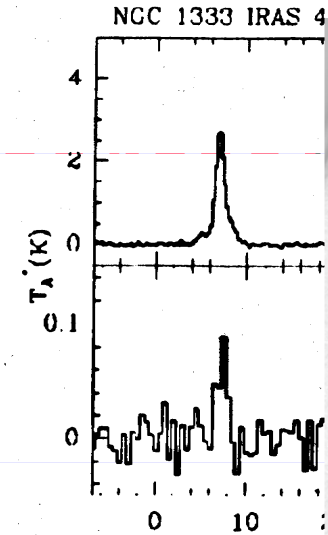

FIG. 1.—Observ
at 372.672 GHz. Th
spectra have been

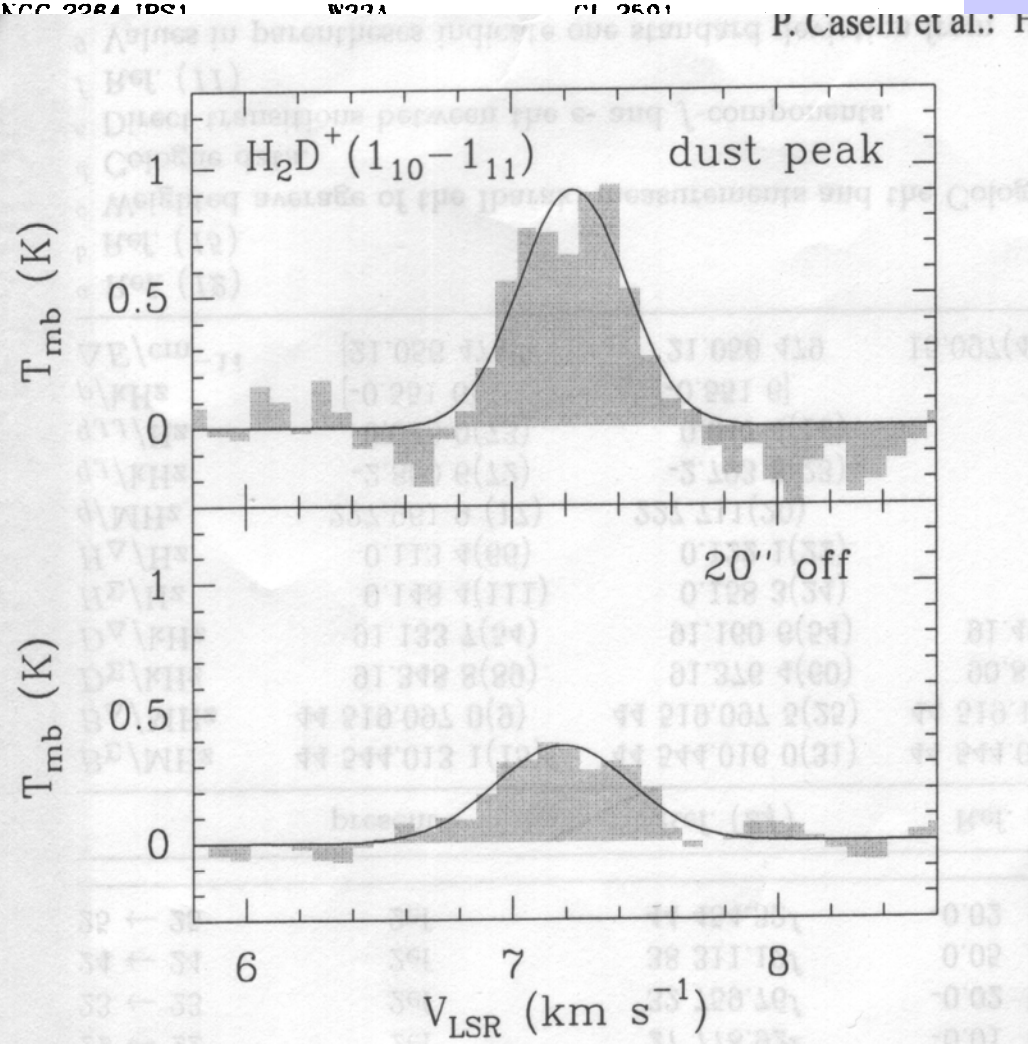

Fig. 1. (*Top*) The $H_2D^+(1_{10}–1_{11})$ line at the dust peak of L1544 (RA(1950) = 05:01:13.1, Dec(1950) = 25:06:35.0). The black curve is the Gaussian fit (see Table 1). (*Bottom*) The $H_2D^+(1_{10}–1_{11})$ spectrum averaged in the four positions 20″ off the dust peak.

Caselli, van d ... 003

D_2H^+ HAS
IN

C. Vastel, T. G. Ph

Ap. J. Lett. **606**

16293E pre-stellar

[D_2H^+] ~ [H_2D^+]

– 10 –

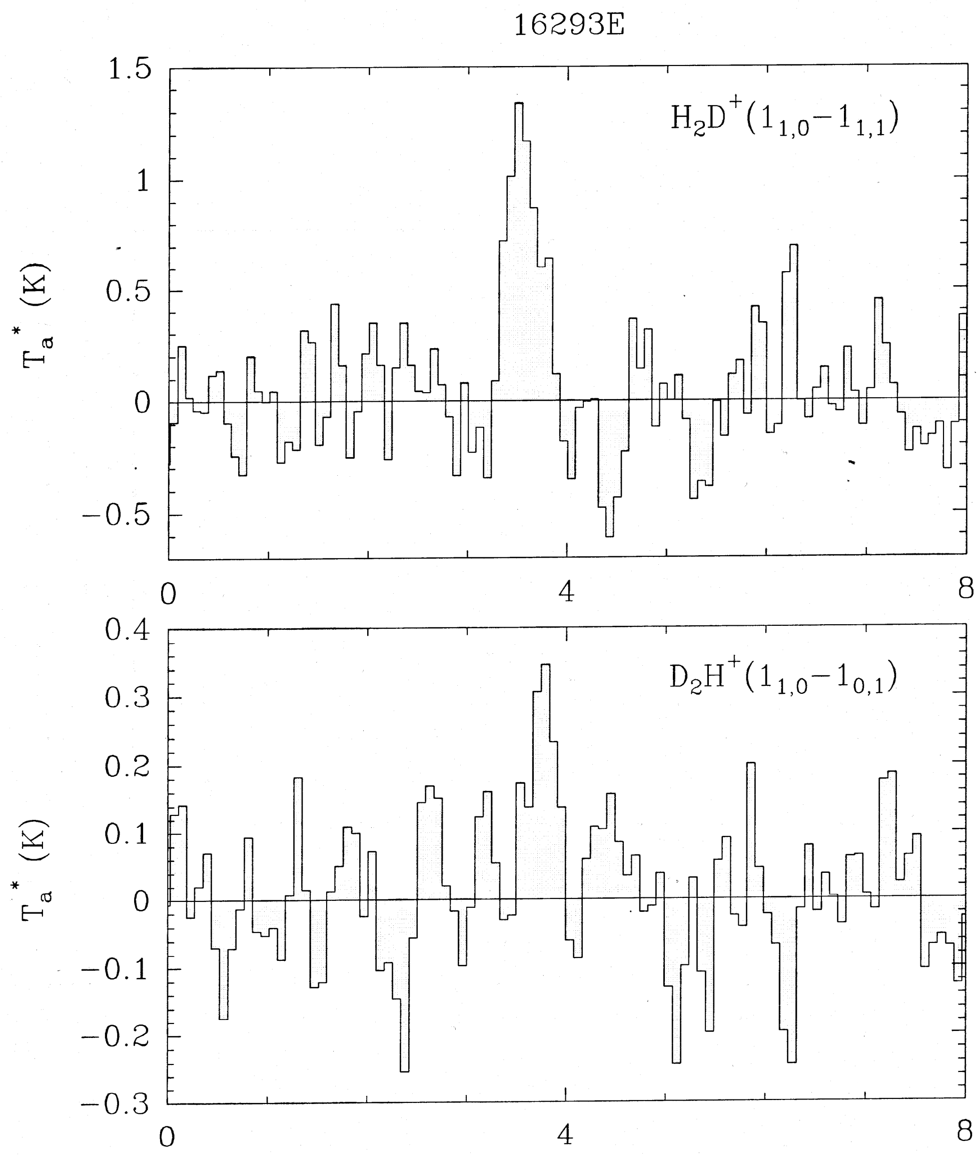

Fig. 3.— Spectra of the ortho-H_2D^+ 1_{10}-1_{11} and para-D_2H^+ 1_{10}-1_{01} transitions towards 16293E.

Table 1. Results of Gaussian fits to the H_2D^+ and D_2H^+ spectra.

Line	ν (GHz)	T_a^* (K)	Δv (km s^{-1})	V_{LSR} (km s^{-1})
H_2D^+ (1_{10}-1_{11})	372.42134(20)[a]	1.31	0.36 ± 0.04	3.55 ± 0.02
D_2H^+ (1_{10}-1_{01})	691.660440(19)[b]	0.34	0.29 ± 0.07	3.76 ± 0.03

[a] Measured frequency by Bogey et al. (1984).

[b] Measured frequency by Hirao and Amano (2003).

⇒ Prompted us to remeasure H_2D^+ line

TuFIR Spectrometer (Toyama University)

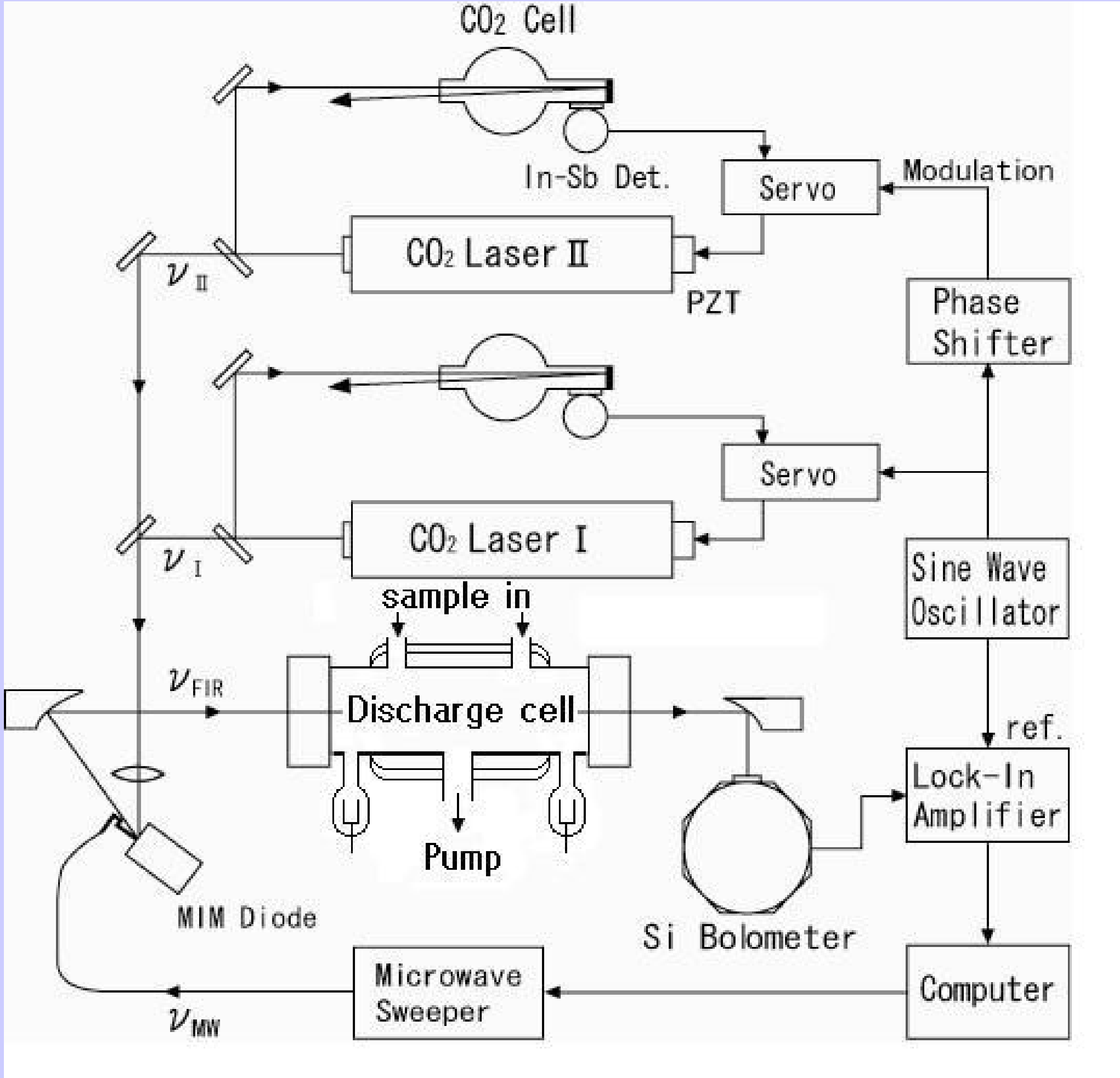

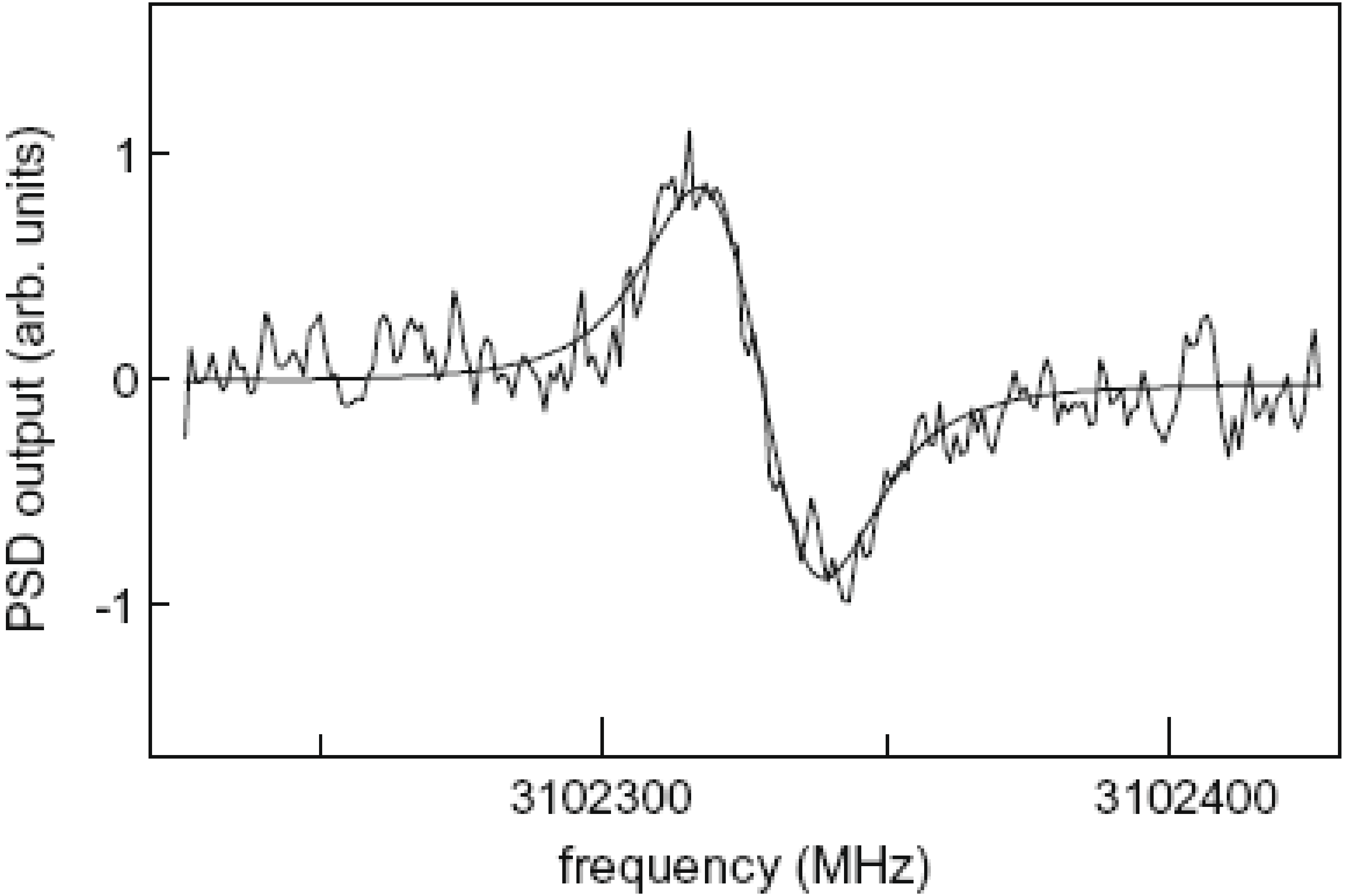

Fig. 1. An example of the observed $2_{11} - 1_{10}$ line at 3.102 THz. The solid line is the first derivative of a fitted Voigt line profile.

Energy Level Diagram of H_2D^+

The Astrophysical Journal, 657: L21–L24, 2007 March 1

hampton et al. (2007). Hence, it is directly related with the line opacity convolved with the instrumental spectral profile of the LWS/FP. The velocity scale in Figure 1 has been obtained assuming λ_{rest} = 126.853 μm (2363.325 GHz), i.e., the wavelength of the o-H_2D^+ 2_{12}–1_{11} transition (Amano & Hirao 2005). The expected error on the frequency of this transition is $\simeq$5 MHz, i.e., a velocity uncertainty <2 km s^{-1} (3 σ), which is much lower than the spectral resolution of the LWS/FP. The p-NH_2 $2_{2,1}$–$1_{1,0}$ J = 5/2–3/2 line is separated by $\simeq -123$ km s^{-1} with respect to the 2_{12}–1_{11} line of o-H_2D^+.

rd
th
e.
al
nt
w
w

line: identification — molecular processes

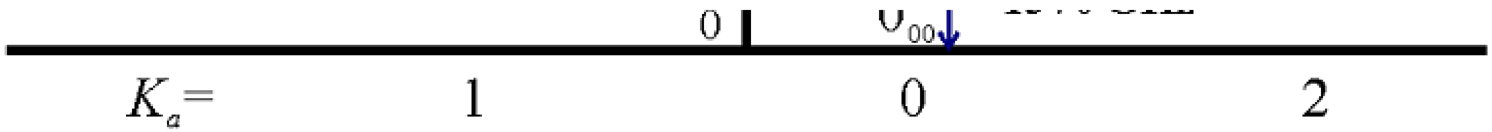

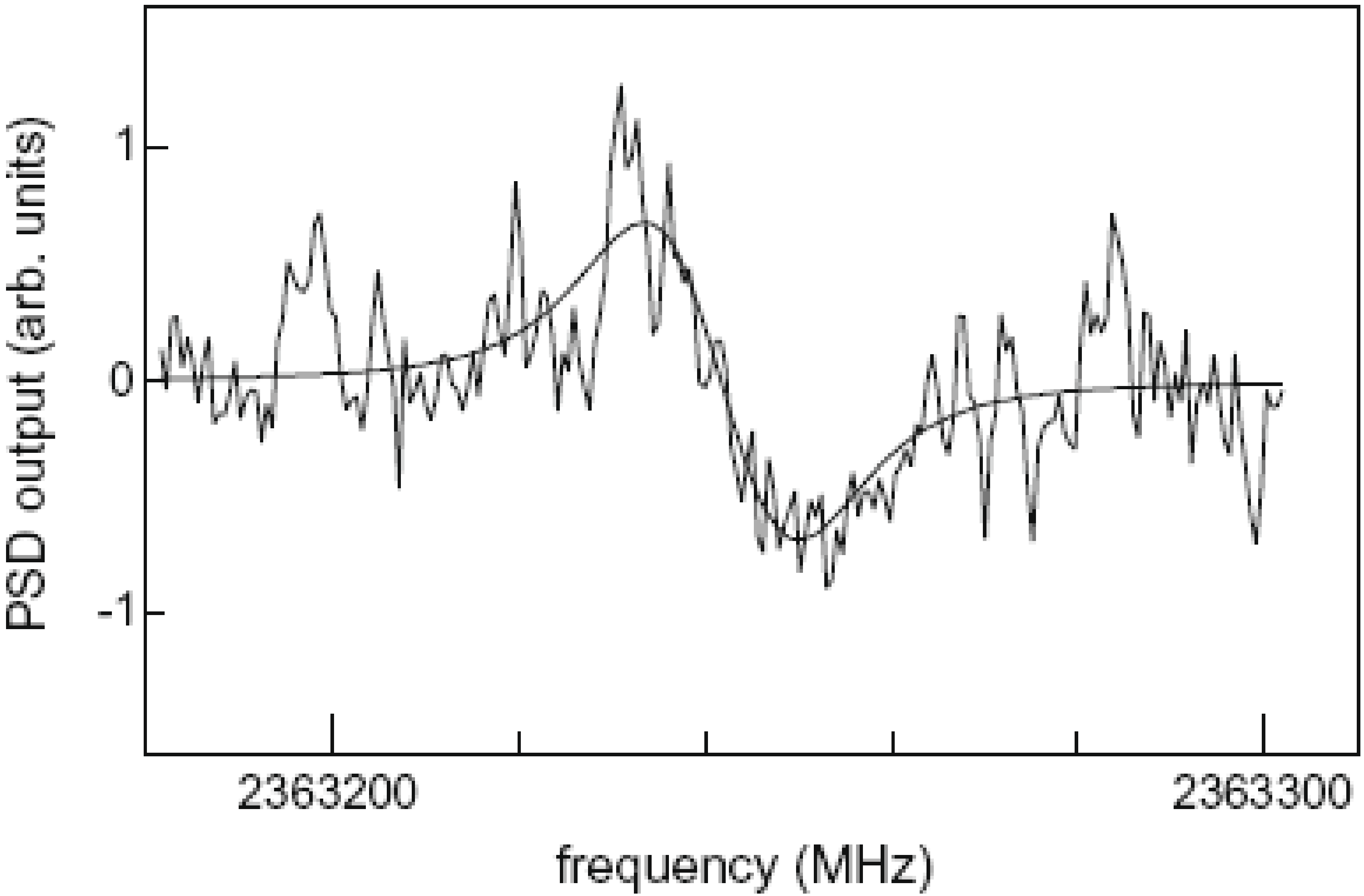

Fig. 2. An example of the observed $2_{12} - 1_{11}$ line at 2.363 THz. The solid line is the first derivative of a fitted Voigt line profile.

Why sub-mm now?

- Ground- and satellite-based astronomical and/or atmospheric observation platforms.
  - Higher spatial resolution with shorter wavelength.
  - Better sensitivity.
- Easy to use laboratory system.
  - multipliers.
  - BWOs.

Atmospheric Opacity in the submillimeter-wave region

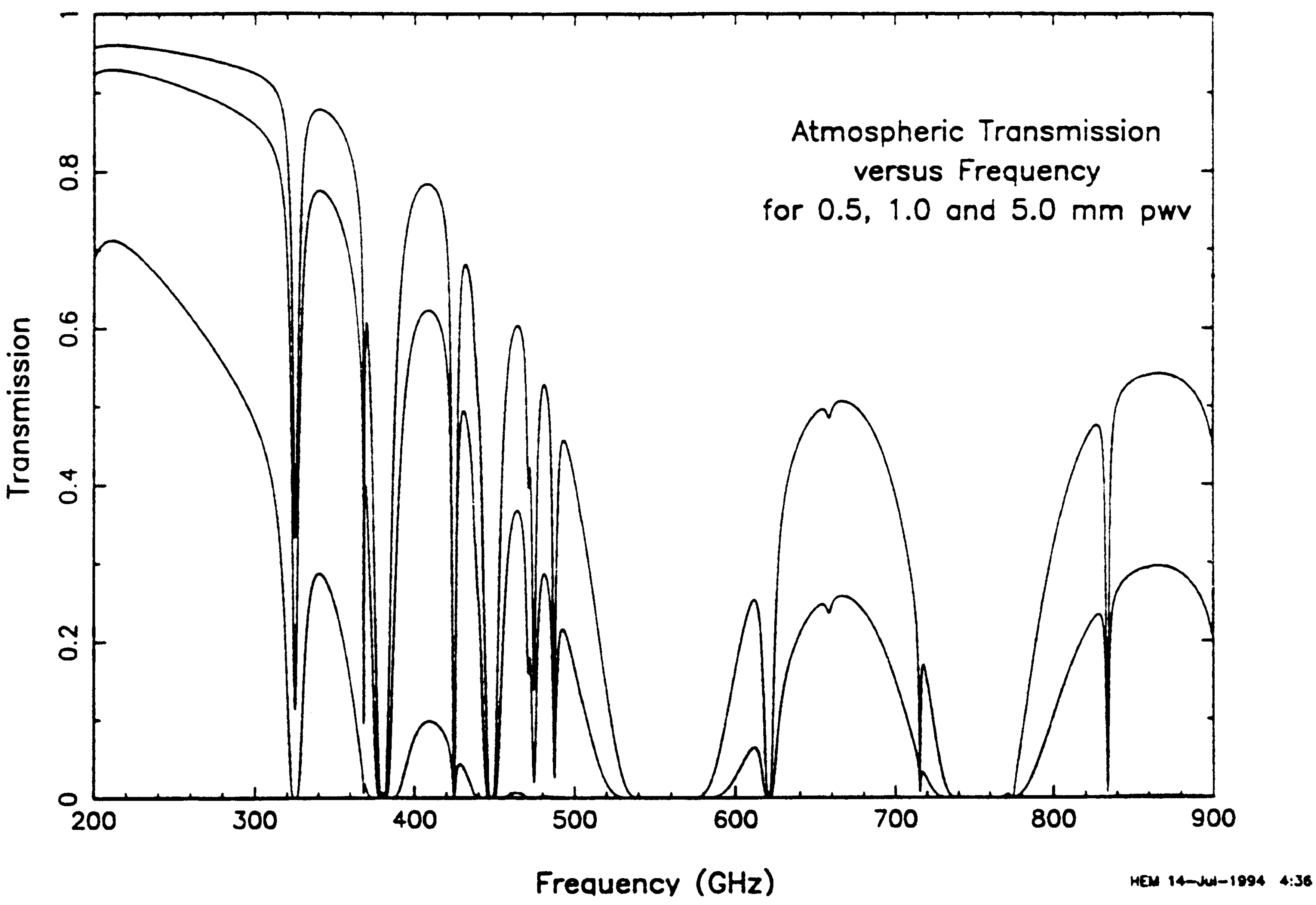

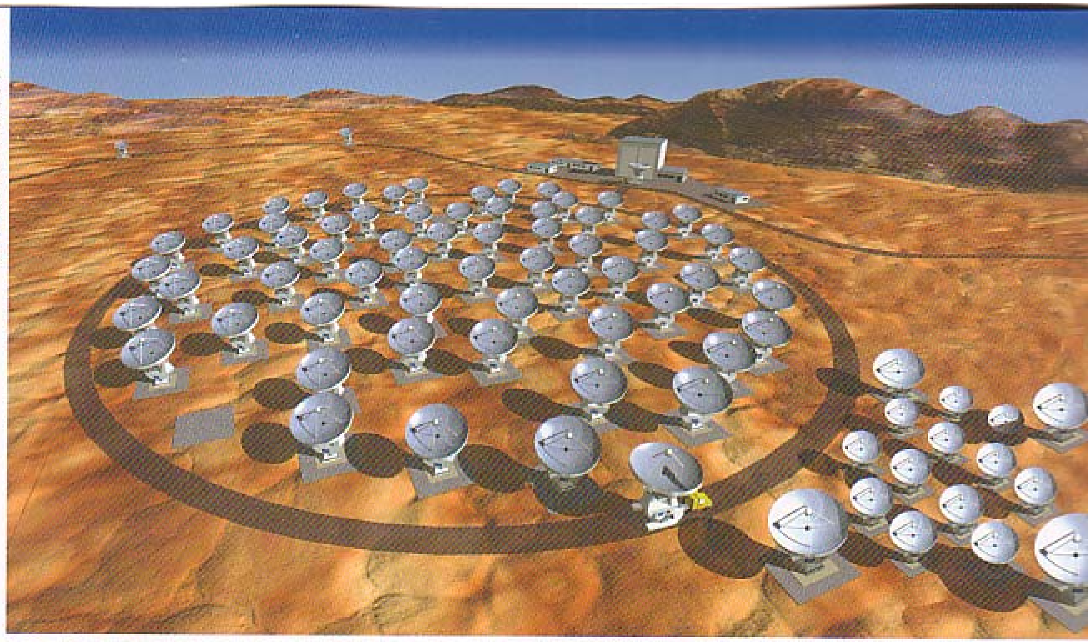

Original CG courtesy of ESO, modified by NAOJ

ALMA(アルマ)は、日本・北アメリカ・ヨーロッパの諸国が協力して、チリ・アンデス山中の標高5000mの高原に建設することを計画している、アタカマ大型ミリ波サブミリ波干渉計(**A**tacama **L**arge **M**illimeter/submillimeter **A**rray)の略称です。直径12mの高精度アンテナ64台と「ACAシステム」と呼ばれる超高精度アンテナ16台からなる、全部で80台のアンテナを干渉計方式で組み合わせ、ひとつの巨大な電波望遠鏡を合成します。電波の中で最も波長が短く、最高の周波数帯である「ミリ波・サブミリ波」を使って、ビッグバン後間もない宇宙初期における銀河の誕生、今も続くさまざまな惑星系の誕生、そして生命につながる物質の進化を解き明かします。

宇宙に一番近い場所

ALMAの設置場所は、チリ共和国北部にあるアタカマ砂漠に近い、アンデス山中の標高約5000mの高原です。世界の候補地を詳しく調査・比較した結果、乾燥した気候、高い標高、平坦な地形、そして安全で容易なアクセスという条件を満たす、この土地が選ばれました。

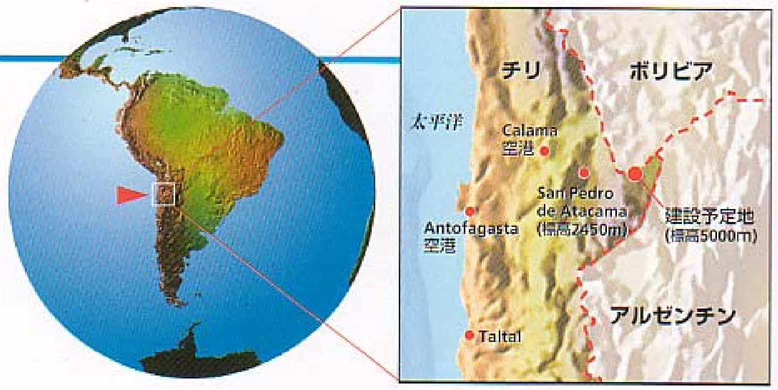

- Visible: dark nebula, heavily obscured by interstellar dust
- Near-IR: dust is transparent, embedded proto-stars can be observed
- Mid- and far-IR: glow from cold dust is directly observable

From NASA web page

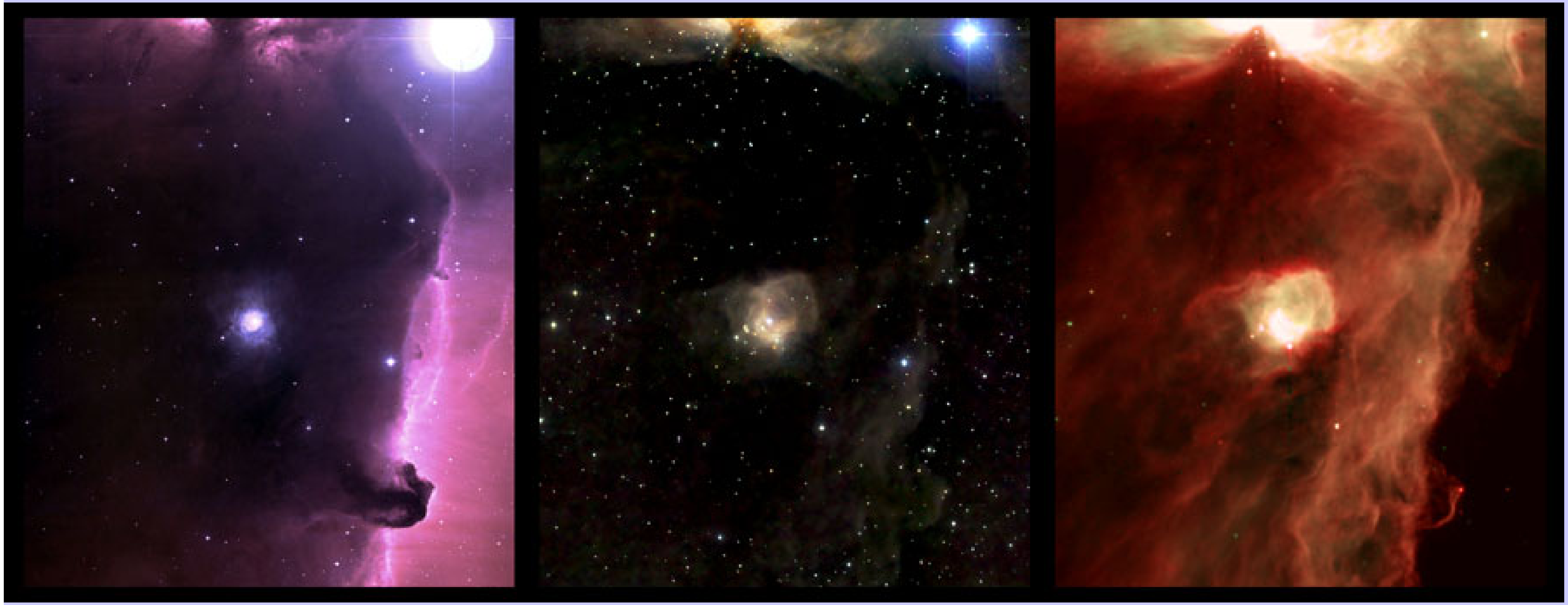

Visible **Near Infrared** **Mid-Infrared**

Getting the WHOLE picture

- An object can look radically different depending on the type of light collected from it:

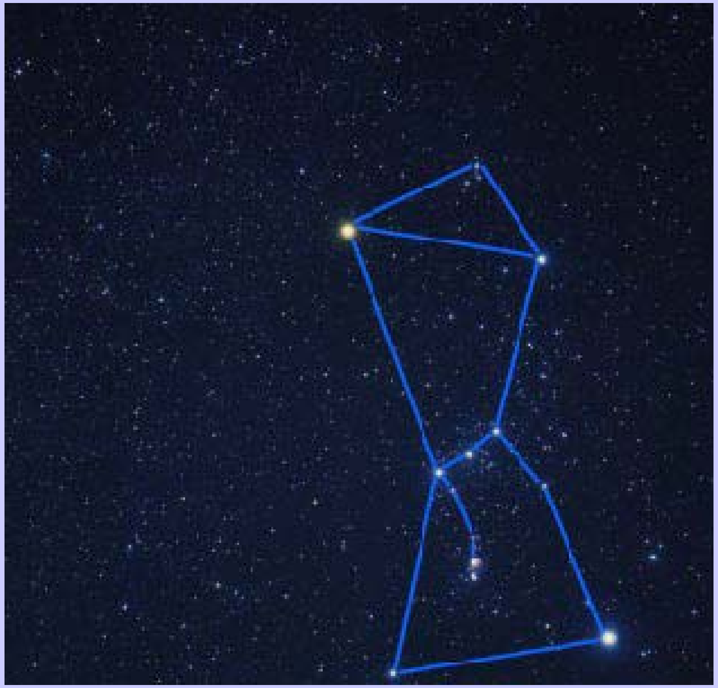

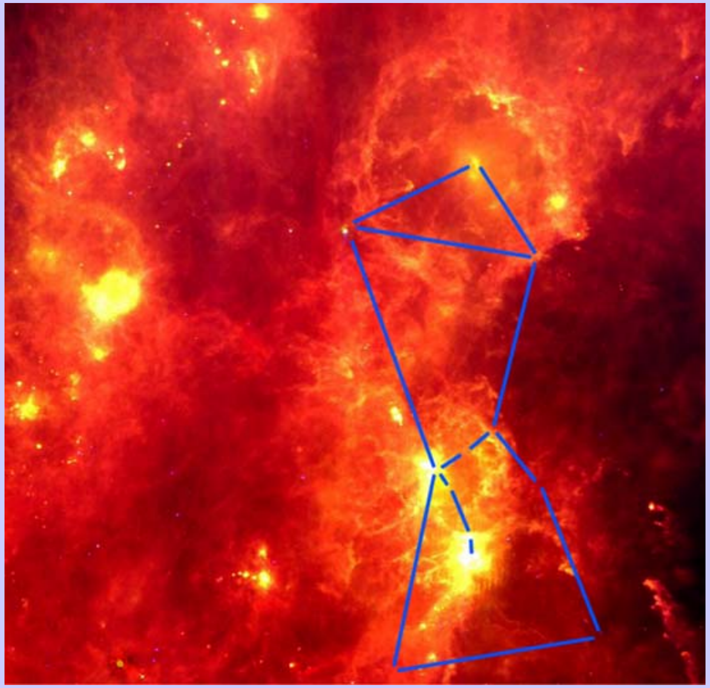

Constellation Orion
left: visual wavelengths
right: far-infrared image

From NASA web page

NASA/DLR

1 mm Survey of Orion with IRAM 30-m Telescope

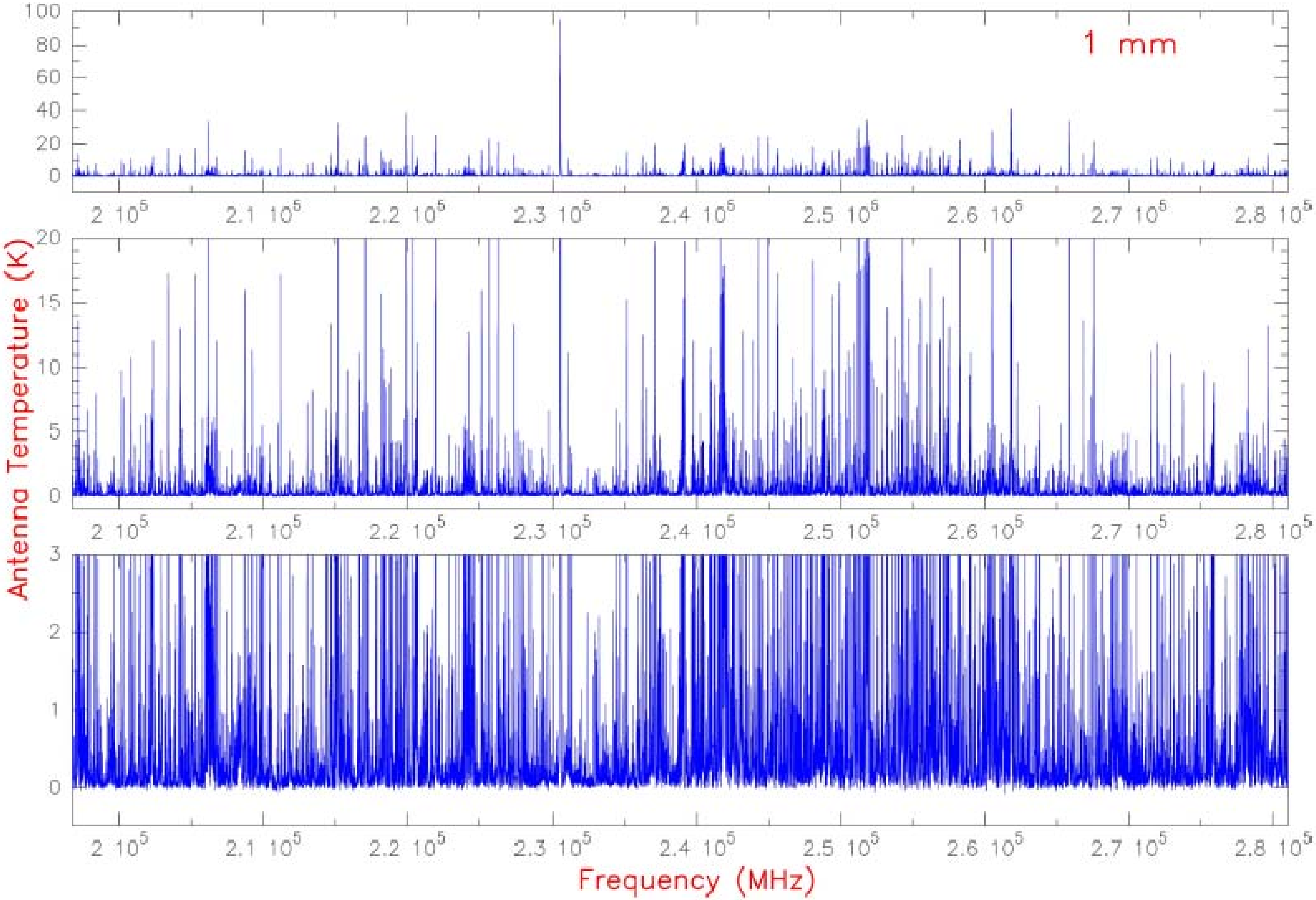

courtesy of J. Cernicharo

In future・・・・・・・

- Sub-mm astronomical observations with very high spatial resolution.

  ALMA

- In the process of star and planet formation, what kind of molecules can survive and be entrained into the planetary system? Life related molecules?
- Lab. data are essential in such identifications.

Thanks............

- NSERC
- Department of Chemistry, University of Waterloo

Hydrogen, light colorless odorless gas,
which given enough time
turns into human being

氢，轻質量　無色 無味的気体，
如果給它足够的時間
它会逐漸演変成今天的人類

Hydrogen Atom

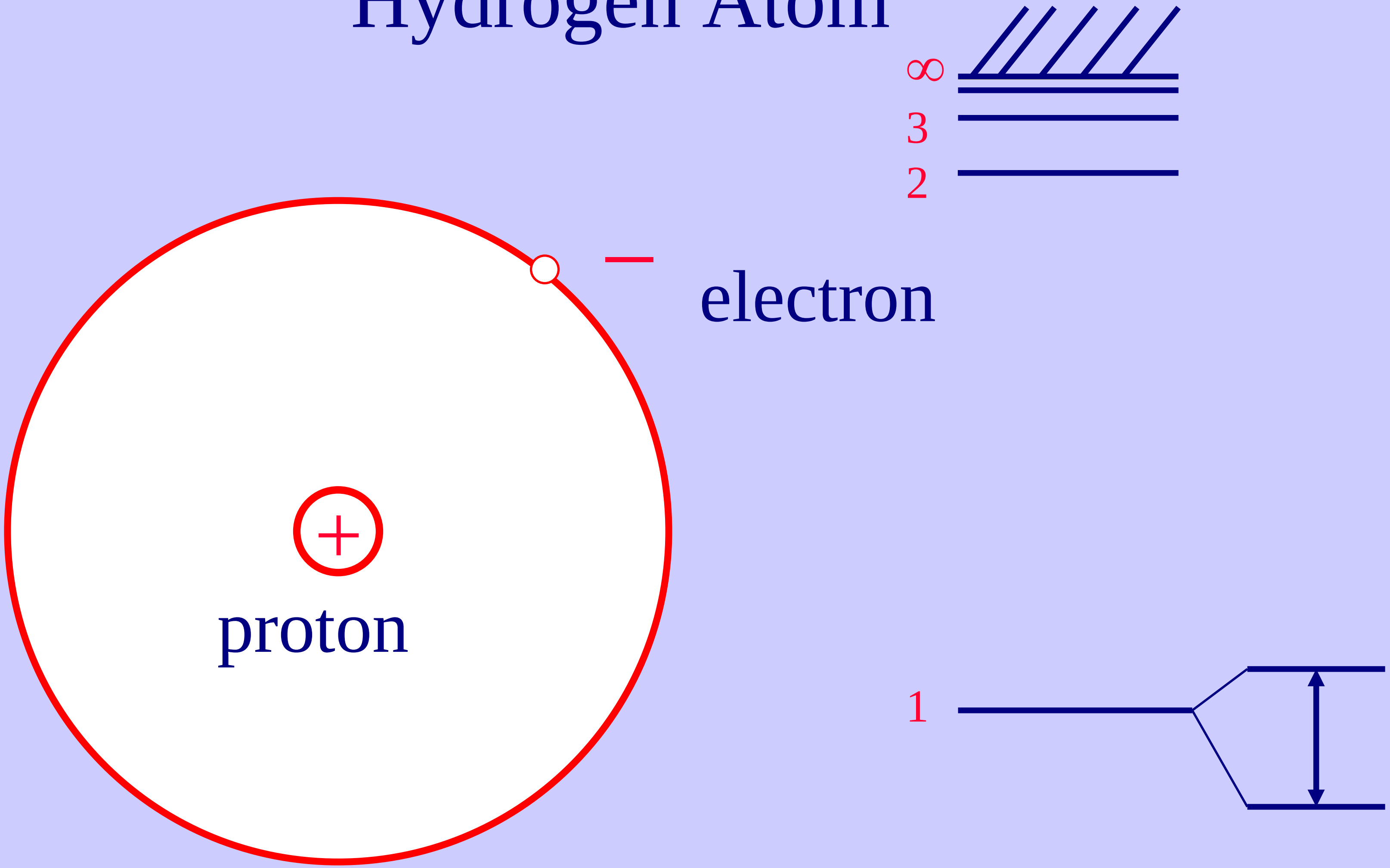

Hyperfine structure
~1.4 GHz, 21 cm

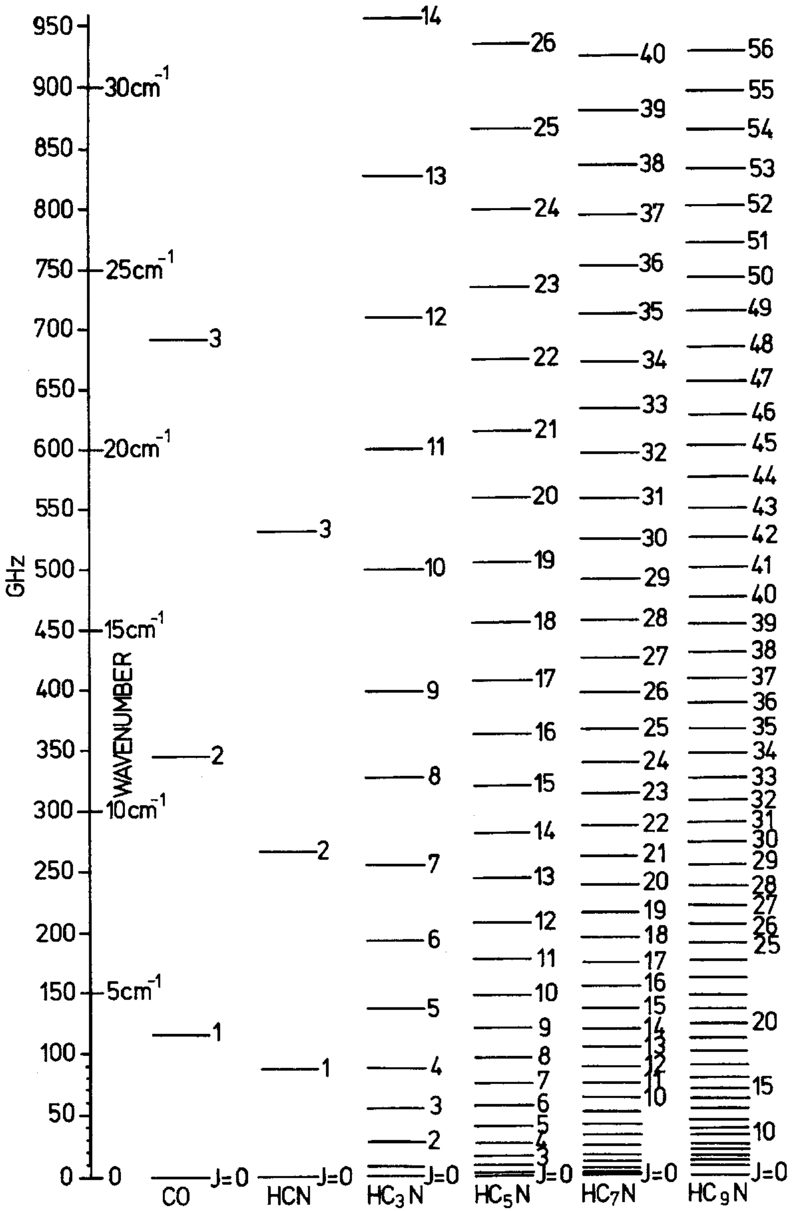

Fig. 13.3. Rotational energy levels of the vibrational ground states of some linear chain molecules detected in the interstellar medium [adapted from Avery (1980)]

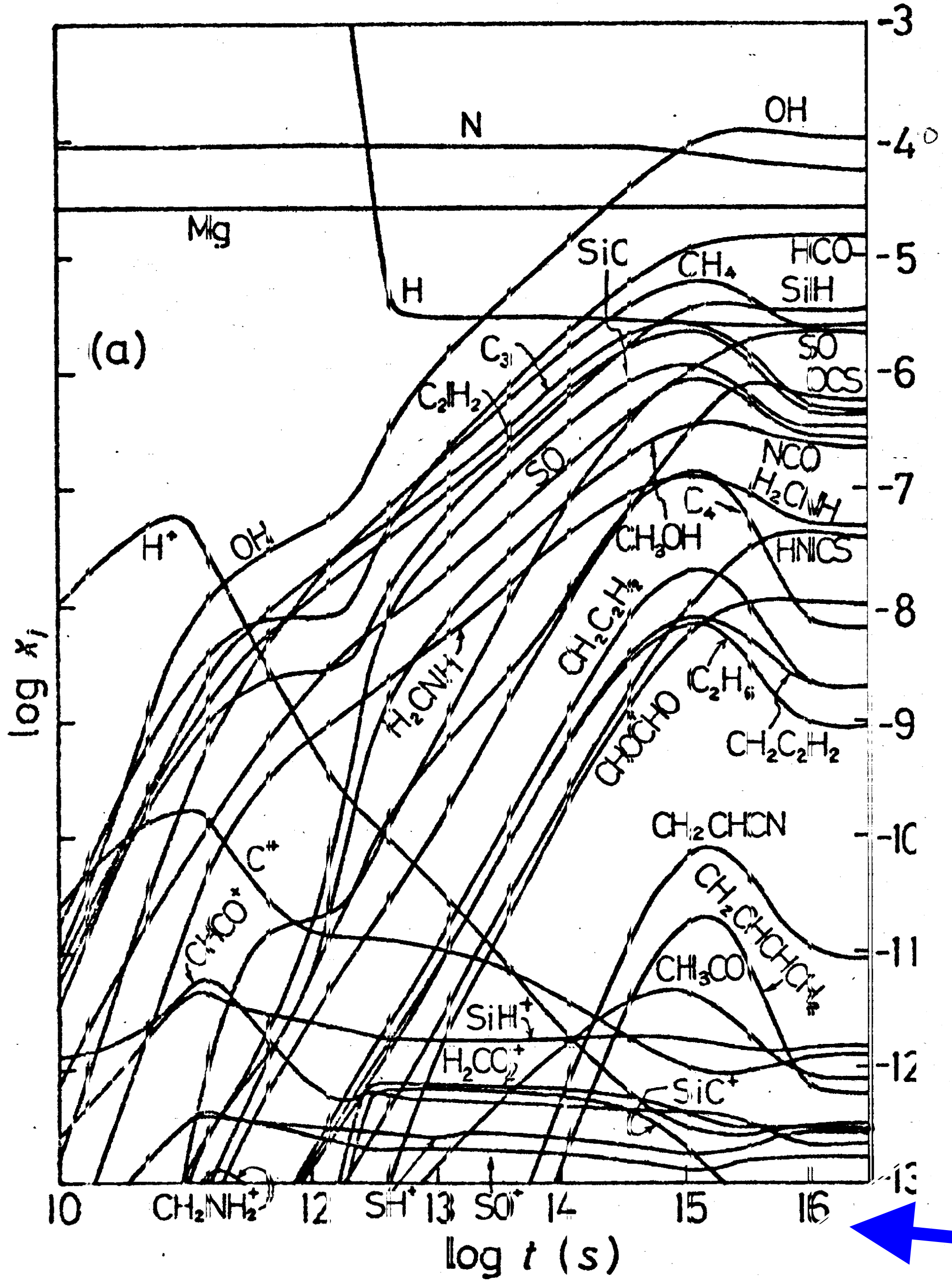

H. Suzuki (鈴木博子)

(1947.7.15~1987.11.22)
1979年.

2234 種の分子種

2885 の反応過程

を取り入れた大規模な計算機シミュレーション

1年＝31557600秒

3．16x10^{7}秒

3．16x10^{8}年

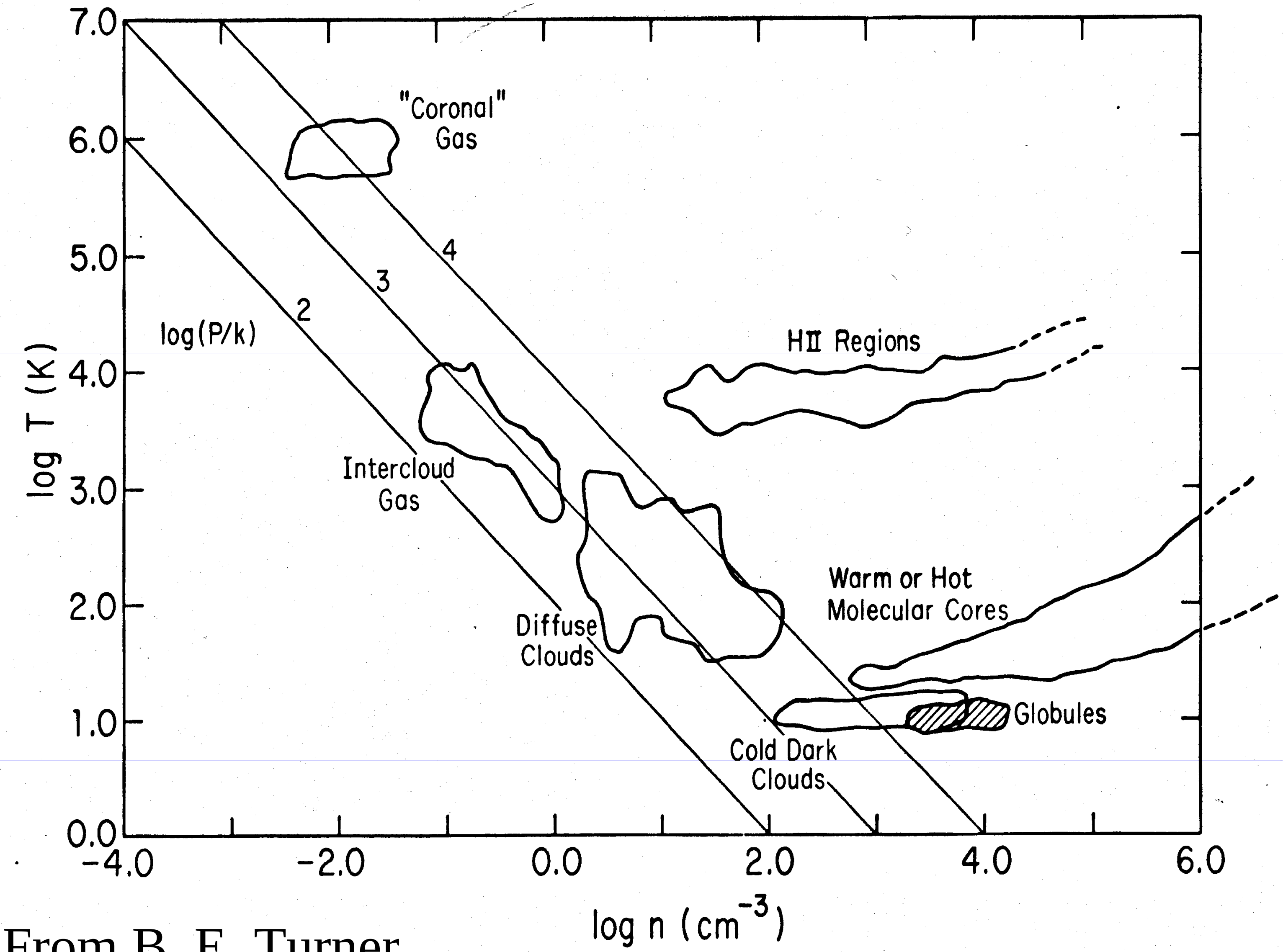

From B. E. Turner

Fig. 4.1. The physical regimes of the interstellar medium, as currently observed.

Conclusion

Submillimeter-wave lines of CN^- and CCH^- have been investigated with BWO based spectrometer.

Extended negative glow discharge and "hollow anode" discharge are good negative Ion sources.

Sub-mm observations of CN^- and CCH^-

- Production of CN^- ;

  C_2N_2 2 mTorr + Ar 12 mTorr in either "hollow anode discharge" or extended negative glow discharge of 5~10 mA, cooled to 210 K.

- Production of CCH^- ;

  C_2H_2 2 mTorr + Ar 12 mTorr

Brünken et al, C_2H_2 (85 %) + Ar (15 %) <15 mTorr
dc discharge current of 150 mA at 120 K.

CCH^- in extended negative glow

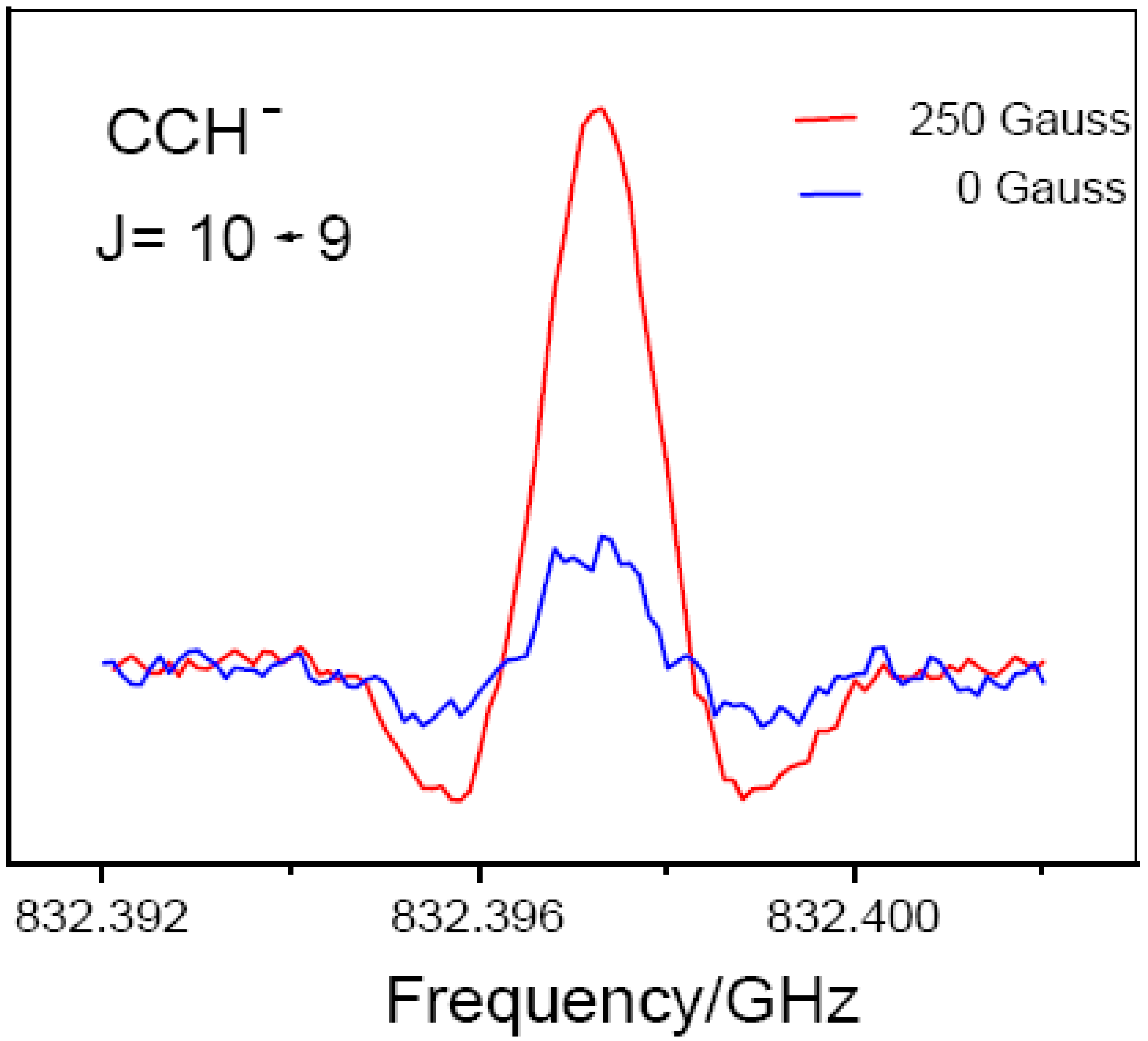

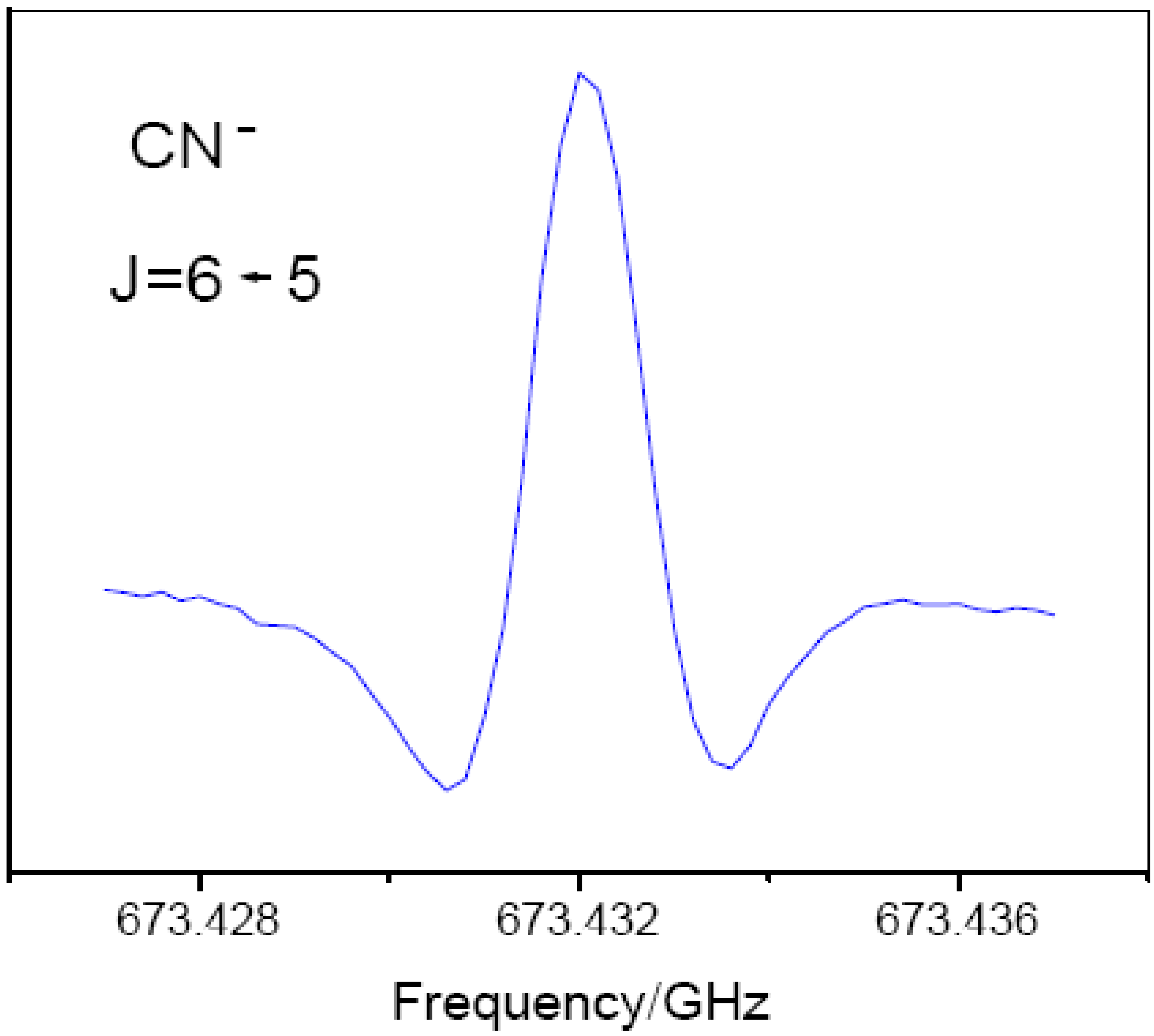

CN⁻
J=6 ← 5
673.428
673.432
673.436
Frequency/GHz

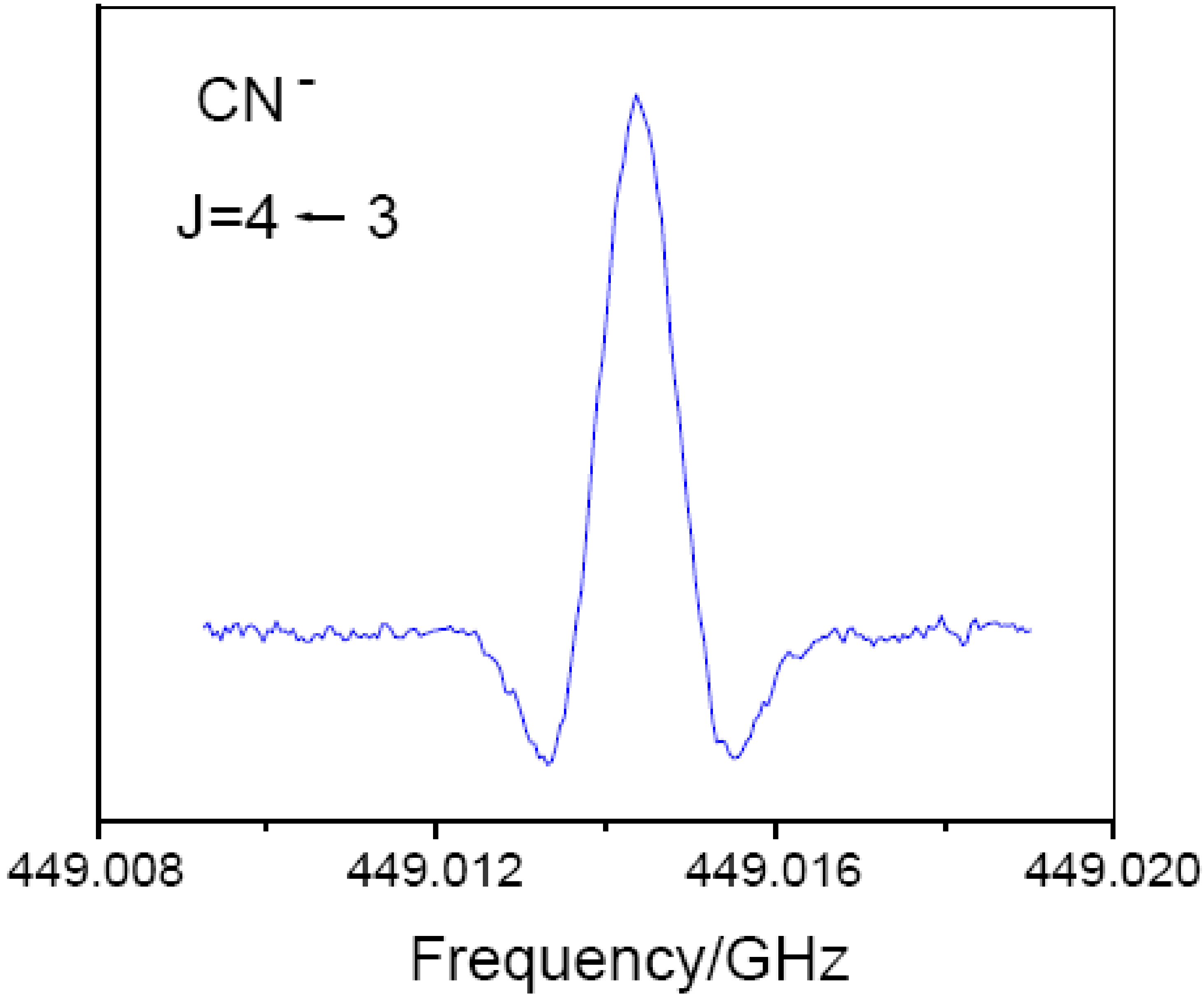

CN $^-$
J=4 ← 3
449.008
449.012
449.016
449.020
Frequency/GHz

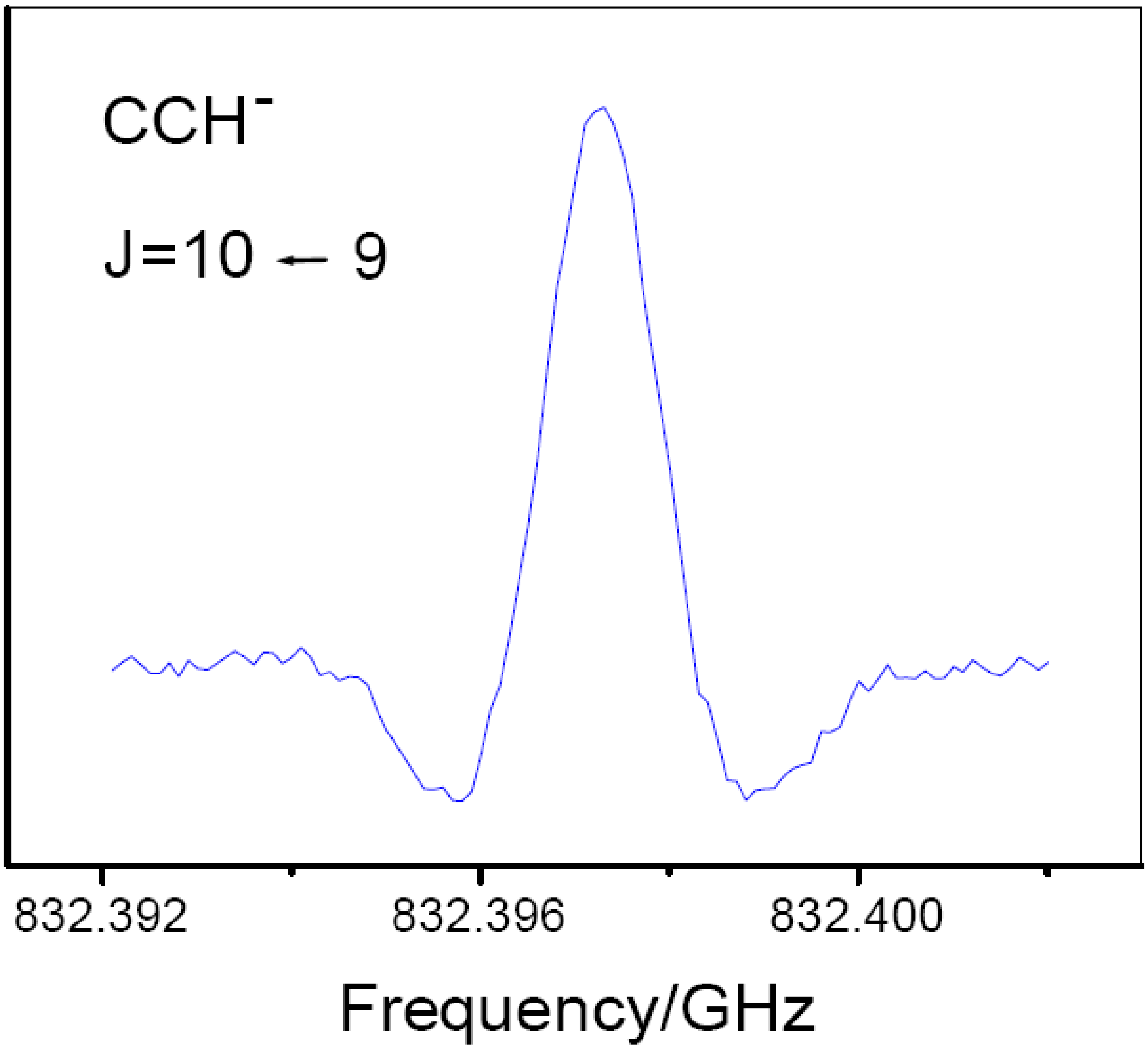

CCH⁻
J=10 ← 9
832.392
832.396
832.400
Frequency/GHz

Observed lines of CN^-

J' – J	*F' – F*	Freq./MHz	Δ /kHz
1 – 0	1 – 1	112263.694	-19
	2 – 1	264.997	21
	0 – 1	266.865	-5
2 – 1	2 – 2	224523.894	101
	1 – 0	523.894	-110
	2 – 1	525.123	67
	3 – 2	525.123	-24
3 – 2		336776.410	11
4 – 3		449014.324	4
5 – 4		561234.330	-14
6 – 5		673422.000	1
7 – 6		785602.811	2

C. A. Gottlieb et al, *J. Chem. Phys*. **126**, 191101(2007)

Fitted Molecular Constants of CN^-

	present	Gottlieb et al
B / MHz	56132.7544(16)	56132.7504(35)
D / kHz	186.6406(22)	185.79(15)
eQq / MHz	-4.230(48)	-4.238(32)

Gottlieb et al, *J. Chem. Phys.* **126**, 191101 (2007)

Observed lines of CCH^-

J' - J	Freq/MHz	Δ/kHz
1 – 0	83278.094	13
2 – 1	166553.865	29
3 – 2	249824.940	0
4 – 3	333089.049	-18
5 – 4	416343.896	2
6 – 5	499587.062	-32
7 – 6	582816.368	23
8 – 7	666029.327	5
9 – 8	749223.698	-5
10 – 9	832397.165	1

Molecular Constants		
B	41639.237(4)	MHz
D	96.97(9)	kHz
H	0.13(fixed)	Hz
B	41639.2341(11)	MHz
D	96.8989(67)	kHz
H	0.13(fixed)	Hz

S. Brünken et al, *Astron. Astrophys*. **464**, L33(2007)

Hollow-anode cell

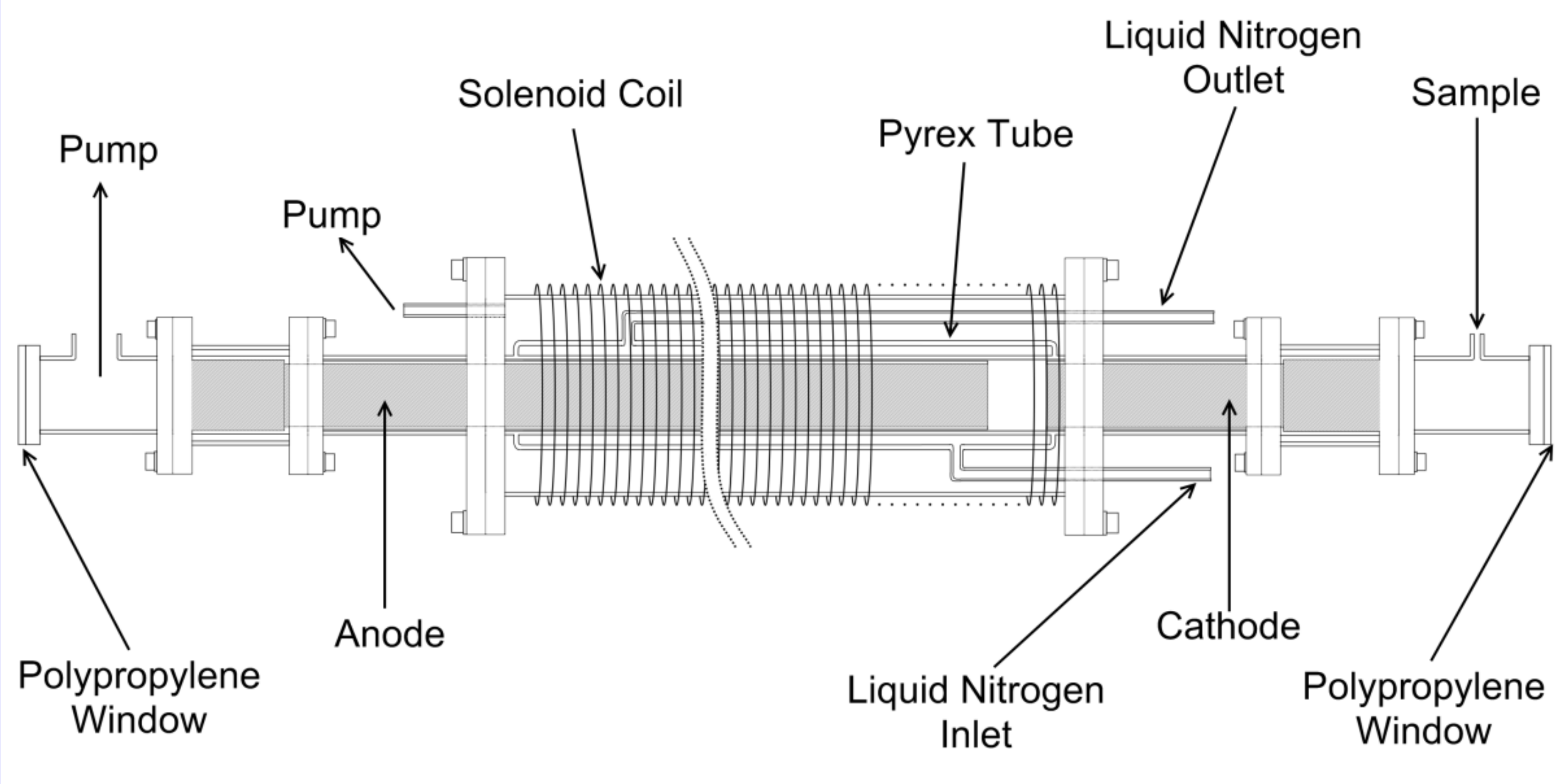

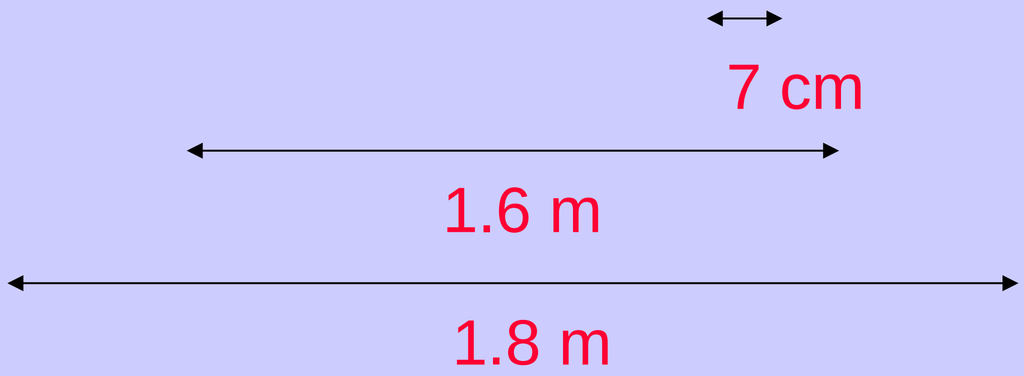

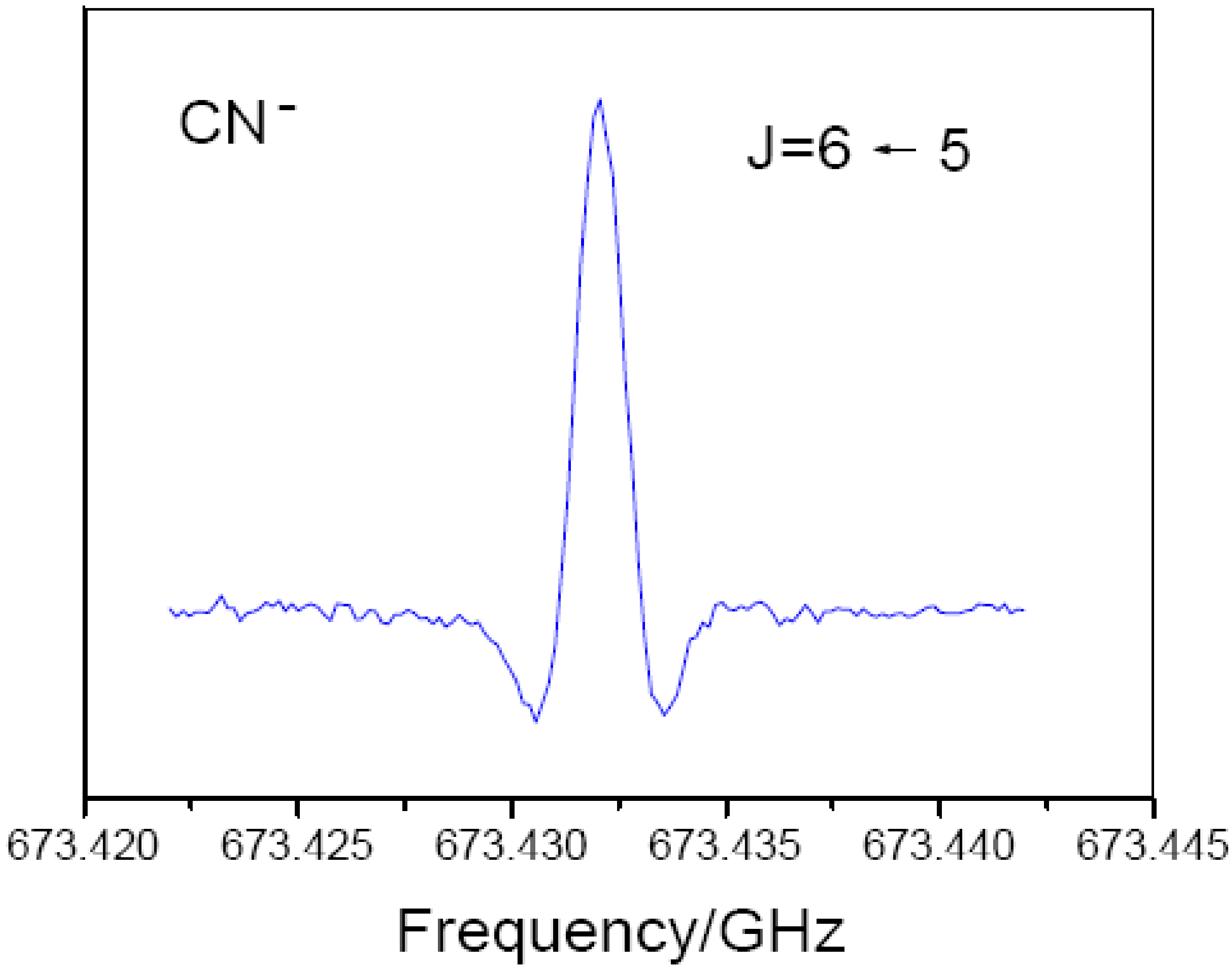

CN⁻
J=6 ← 5
673.420
673.425
673.430
673.435
673.440
673.445
Frequency/GHz

CN^- in “hollow anode” discharge

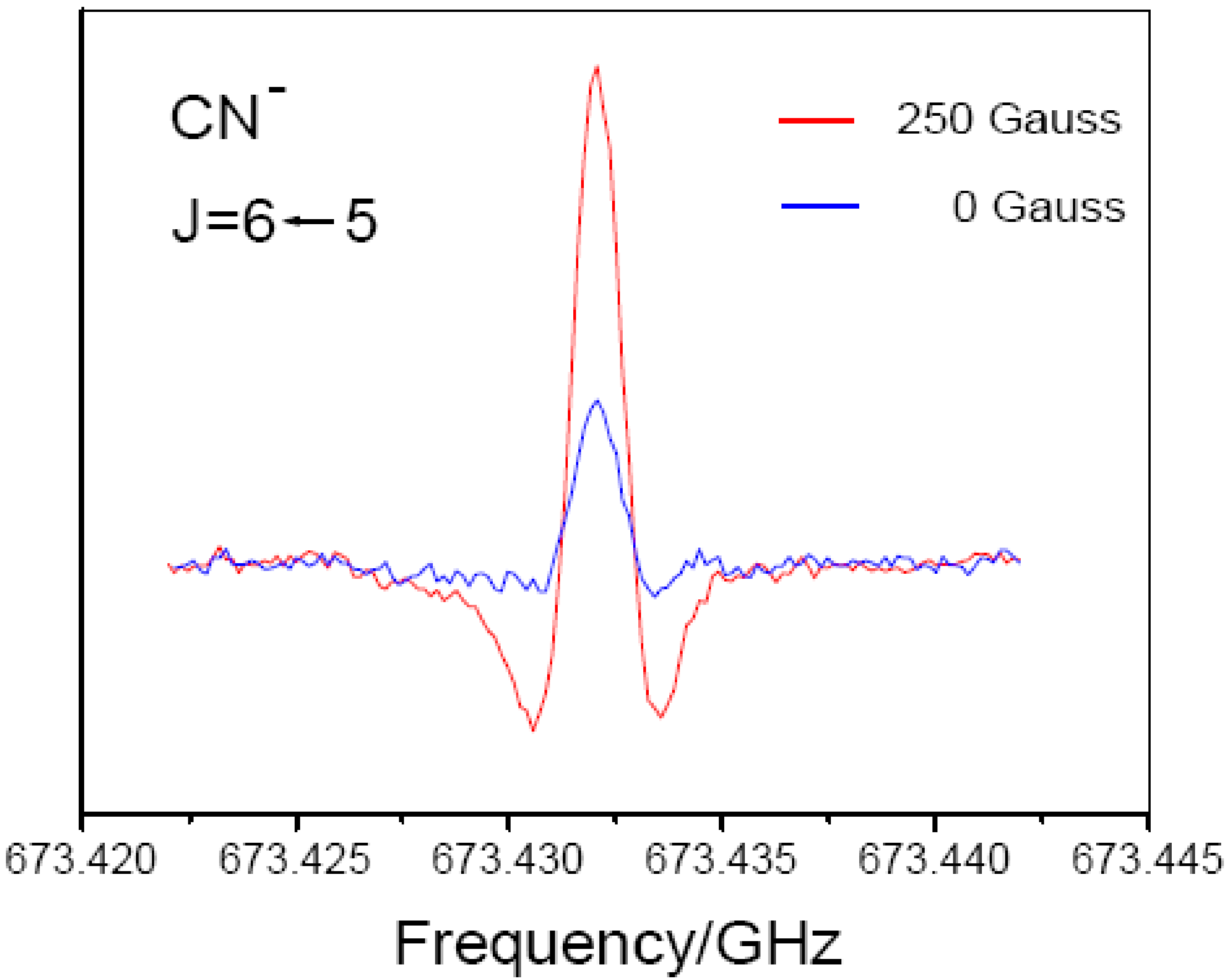

C_4H^- in extended negative glow discharge

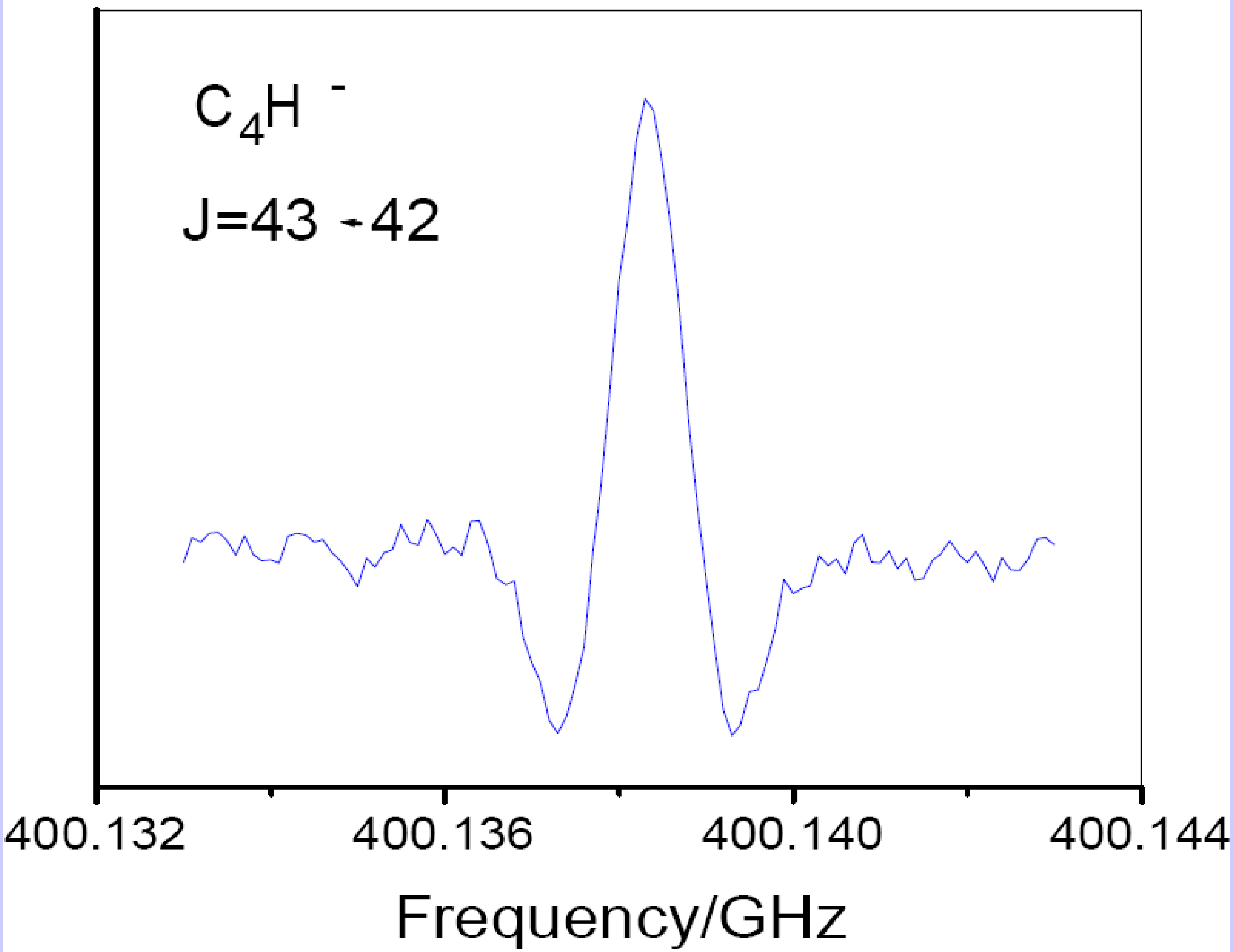

Sub-mm observations of C_3N^-

- Production ;

  C_2N_2 ≤1 mTorr + C_2H_2 ~2 mTorr + Ar 12 mTorr
  in either
  "hollow anode discharge" or
  extended negative glow discharge
  of 4~10 mA, cooled to 210 K.
  Freq. range ~ 504 GHz

Thaddeus et al, HC_3N (20 %) + Ar (80 %) ~15 mTorr
dc discharge current of 20 mA at 200 K.

Extended Negative Glow

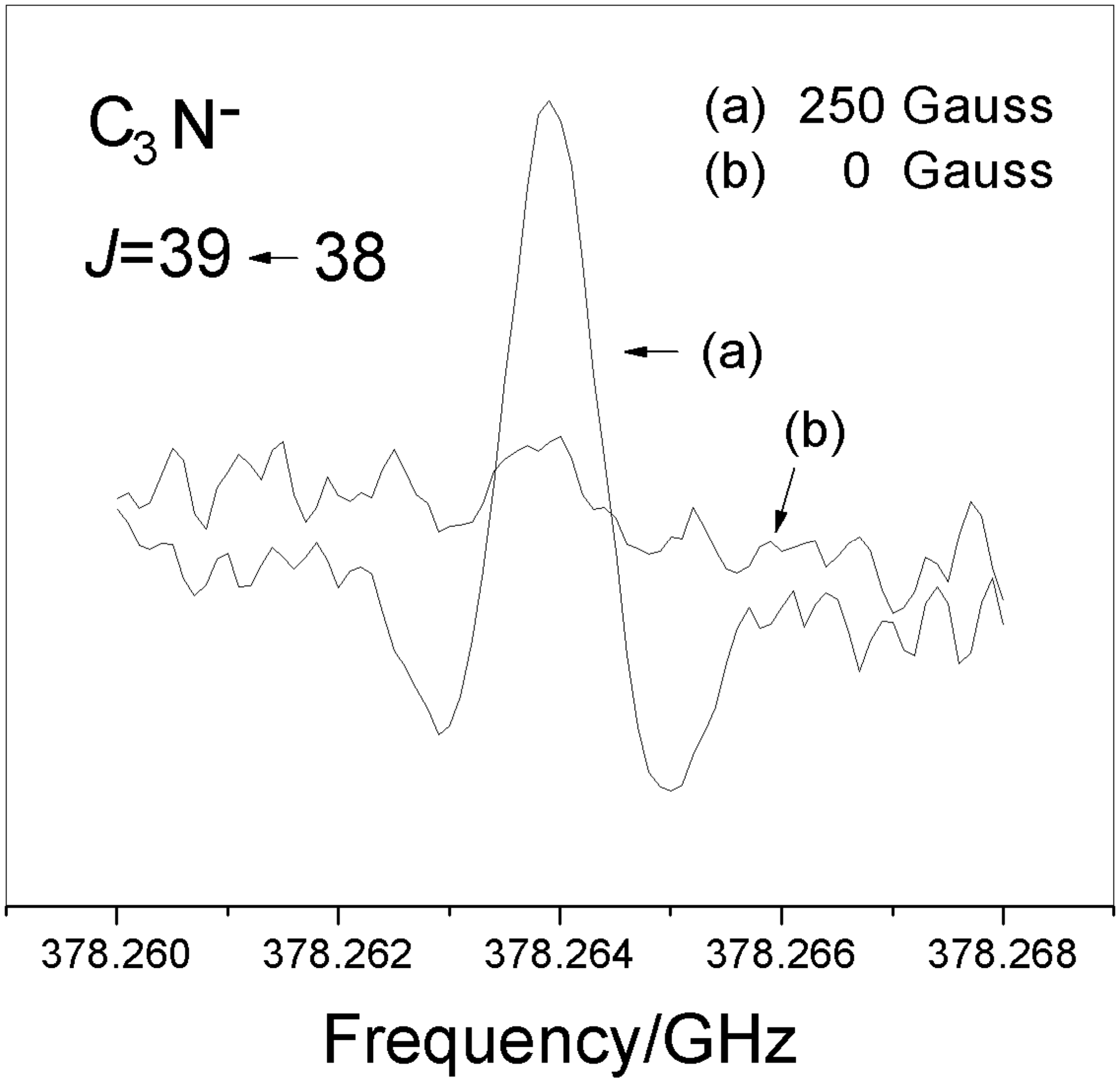

Hollow-anode discharge

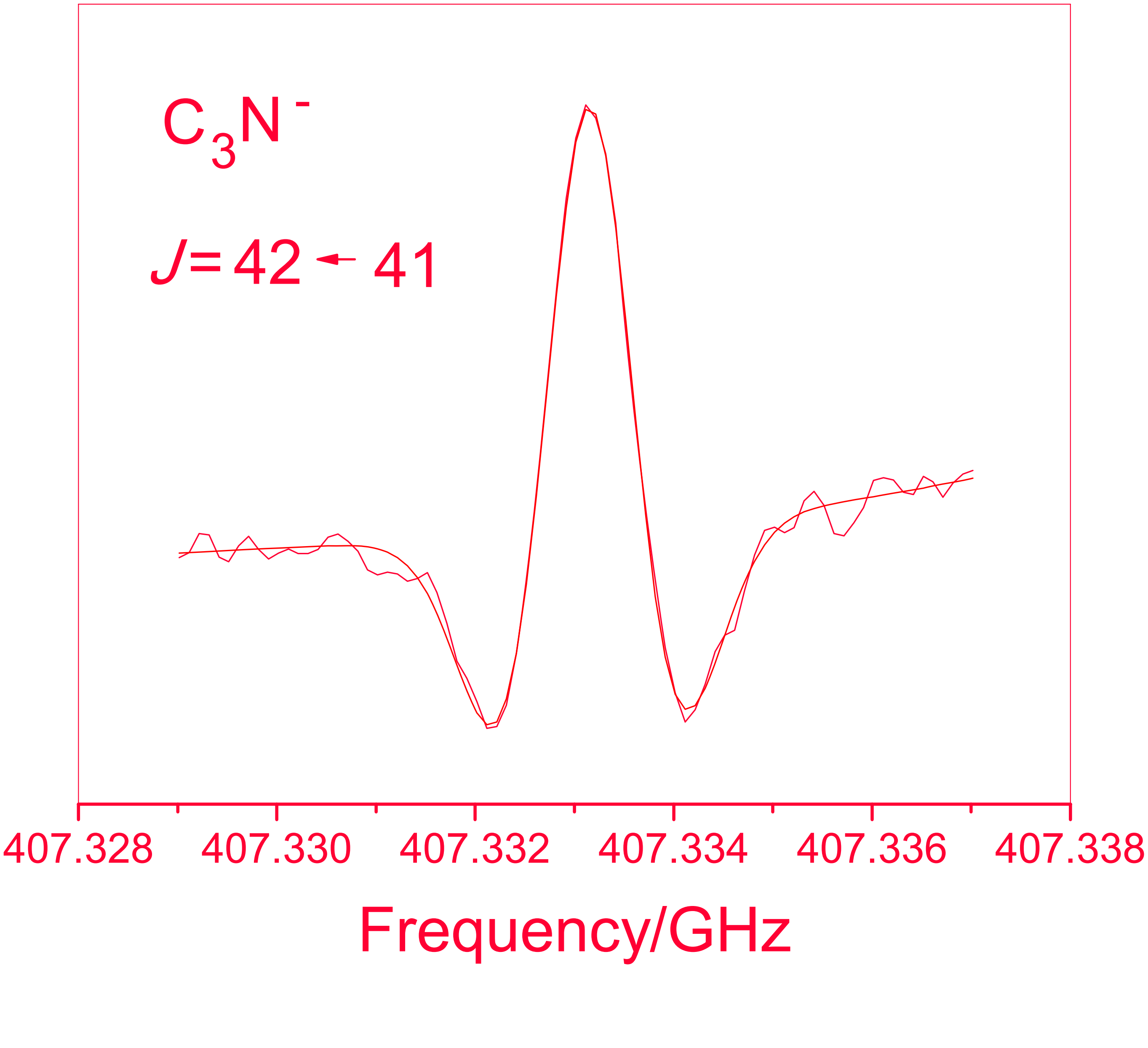

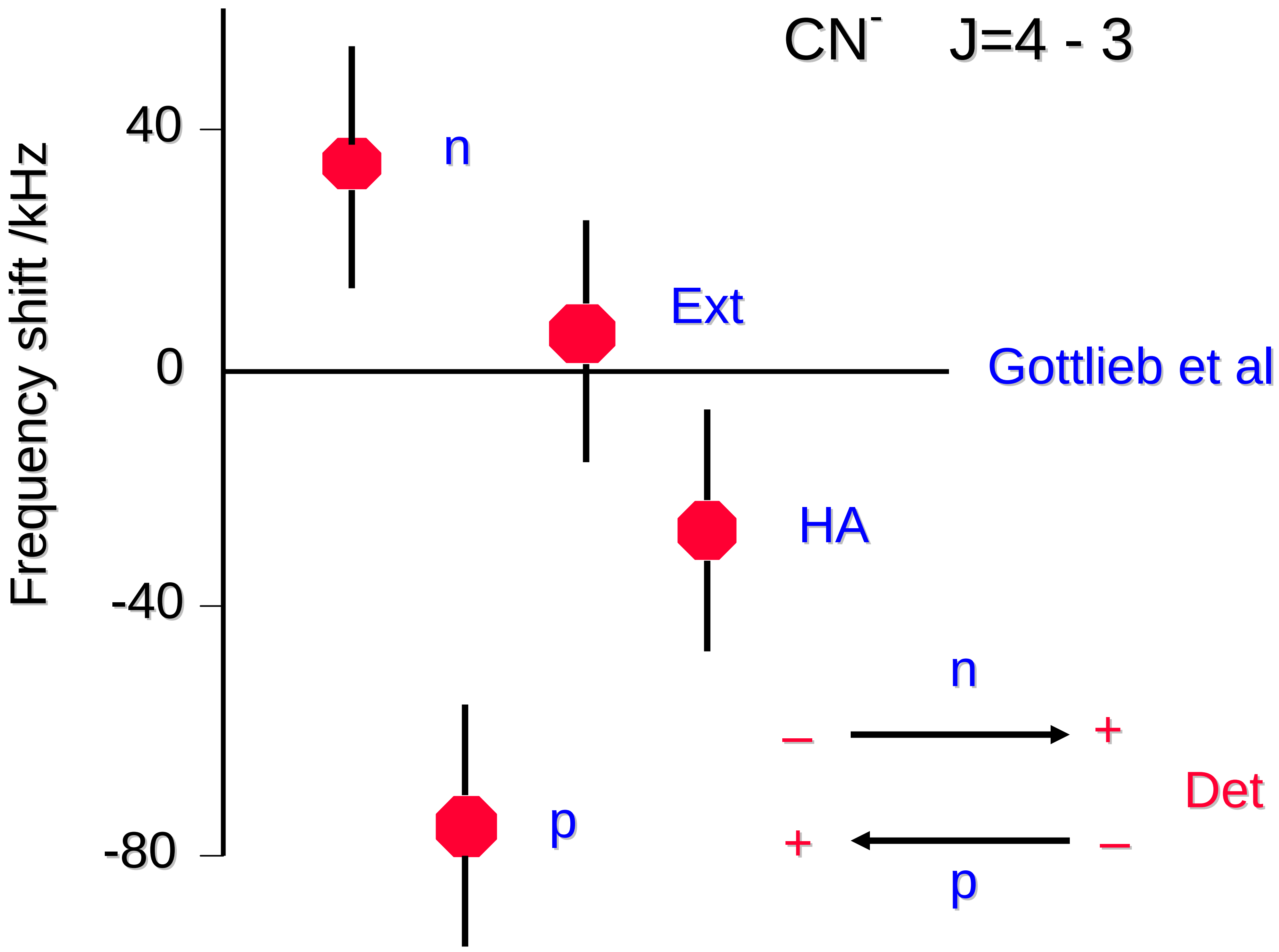

CN⁻ J=4 - 3
Frequency shift /kHz
40
0
-40
-80
n
Ext
Gottlieb et al
HA
p
n
–
+
Det
+
–
p

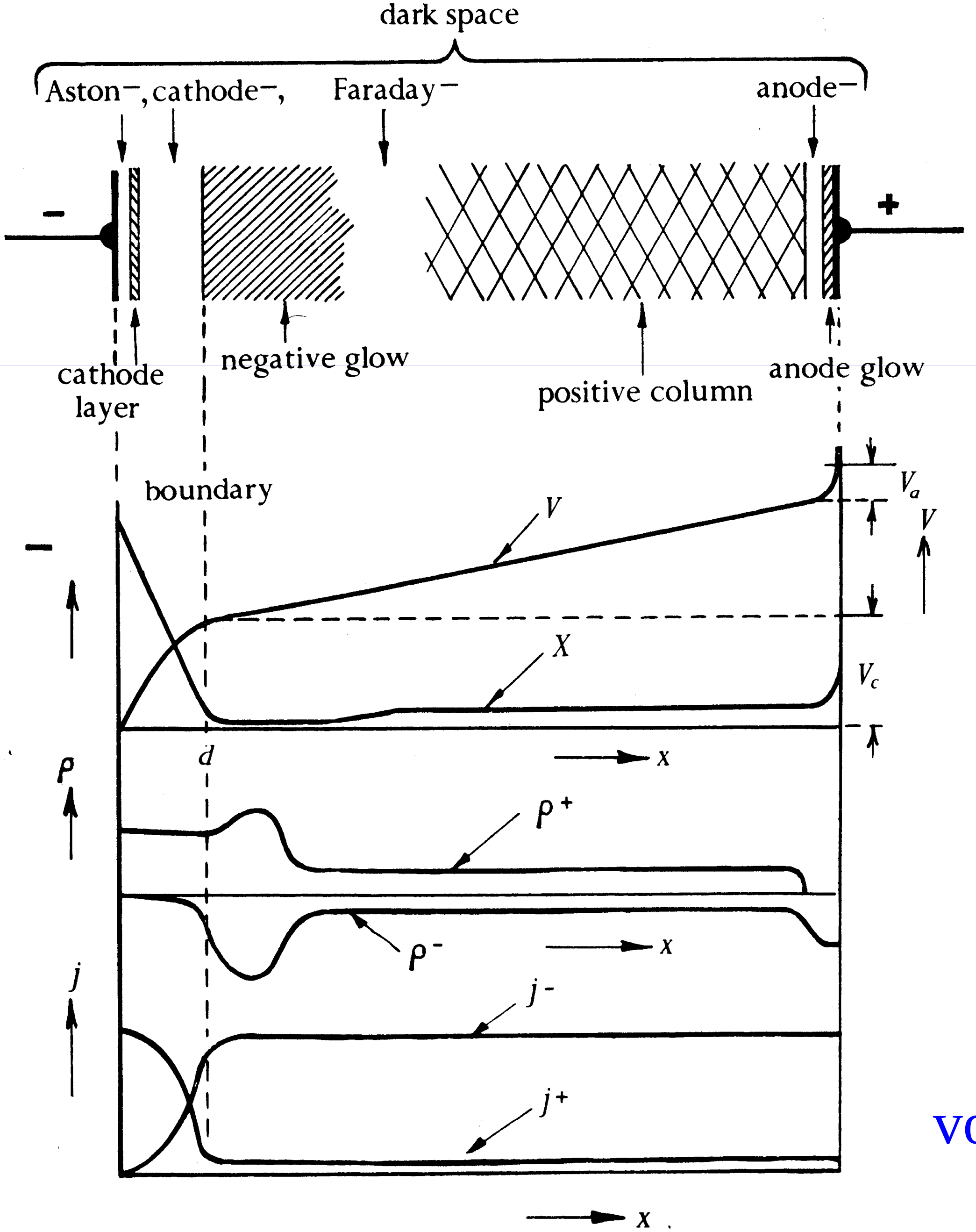

Density of negative charges is high in negative glow and anode glow

von Engel “Ionized Gases”

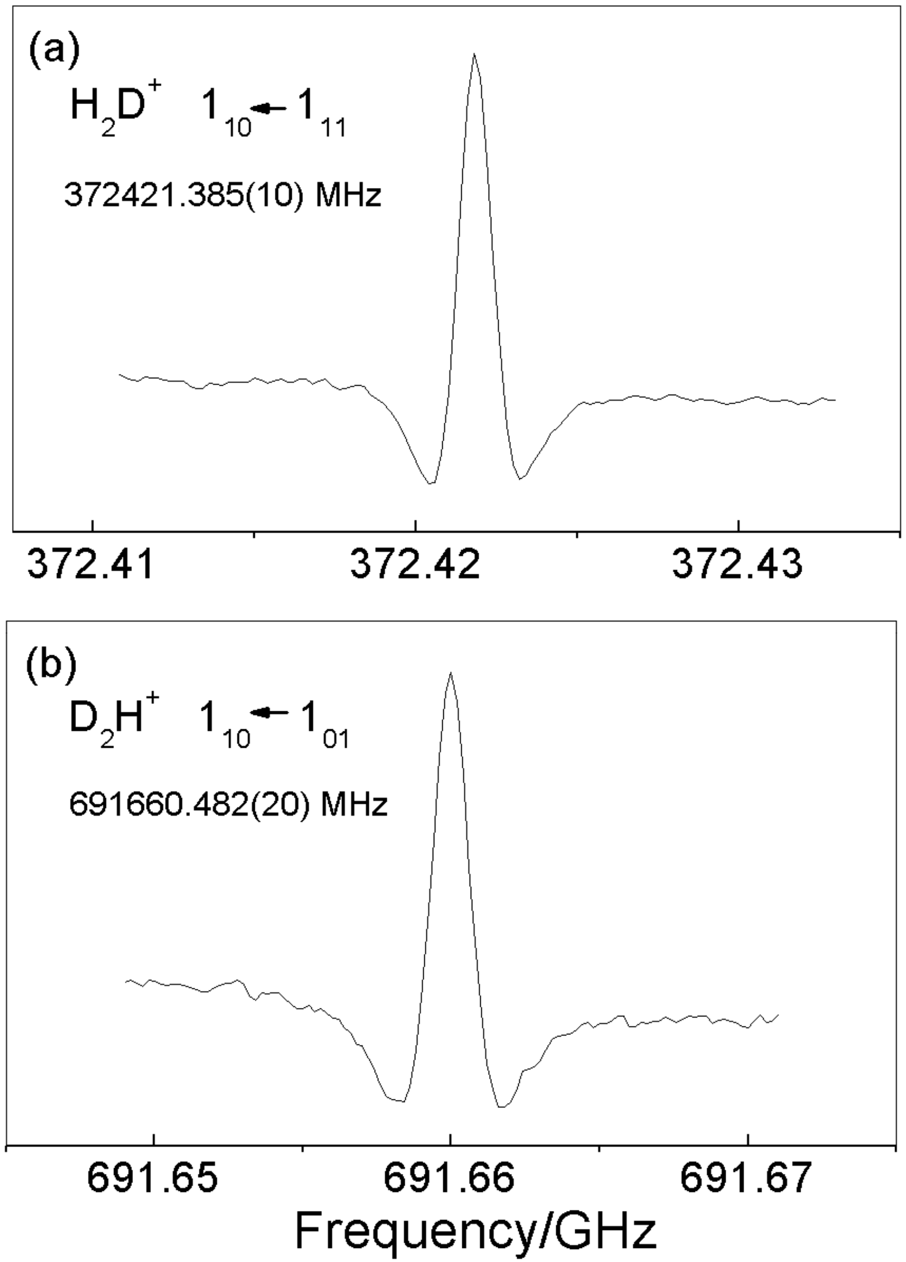

T. Hirao and T. Amano,
Astrophys. J. Lett. ***597****, L85(2003).*

T. Amano and T. Hirao,
J. Mol. Spectrosc. ***233****, 7 (2005).*